

THESIS FOR THE DEGREE OF LICENTIATE OF ENGINEERING

Aspects of building geometry and powder
characteristics in powder bed fusion

ALEXANDER LEICHT



CHALMERS

Department of Industrial and Materials Science
CHALMERS UNIVERSITY OF TECHNOLOGY
Gothenburg, Sweden 2018

Aspects of building geometry and powder characteristics in powder bed fusion
Alexander Leicht

© Alexander Leicht, 2018

Technical report no. IMS-2018-1

Department of Industrial and Materials Science
Chalmers University of Technology
SE-412 96 Gothenburg
Sweden
Telephone + 46 (0)31-772 1000

Printed by Chalmers Reproservice
Gothenburg, Sweden 2018

Aspects of building geometry and powder characteristics in powder bed fusion

Alexander Leicht

Department of Industrial and Materials Science
Chalmers University of Technology

Abstract

Additive manufacturing (AM) produces near-net-shaped parts directly from a 3D-CAD model in a layer-by-layer manner. One of the most common AM technique for fabricating metallic components is powder bed fusion (PBF). The PBF process has shown great potential in fabricating metallic parts with properties better or comparable to conventional methods. However, there are some challenges in reproducibility, process stability, robustness, etc. This thesis elaborates on several of these challenges and addresses the influences of feedstock material, build orientation and part design on the final outcome.

The PBF process uses fine metal powder as feedstock material and in order to have an economically feasible process, powder recycling is a necessity. However, to ensure a robust process and consistent material properties, the feedstock material need to be handled with caution as powder properties will affect the part quality. The obtained results for 316L stainless steel from this study indicate that powder degradation in terms of surface product changes occurs when the powder is recycled. It was revealed that both recycled and virgin powder were covered by a heterogeneous oxide layer, composed by a homogeneous iron oxide layer with the presence of Cr-Mn-rich oxide particulates that were growing during PBF processing. The results showed that the powder degradation was more pronounced when used in the electron beam system compared to a laser based system due to the long exposure at high temperatures.

The manufacturing capabilities of the PBF process has enabled the production of lattice structures without extensive tooling. The properties of such lattice will be influenced by the microstructure. Hence, it is of importance to understand how the part geometry would affect the microstructure. This study presents the effect of build geometry, as e.g. wall thickness and build angle on the 316L microstructure. The obtained results indicated that in the center of ribs over 0.6 mm in thickness, large elongated grains with preferential $\langle 101 \rangle$ orientation were created. Reducing the part thickness to below 0.6 mm reduced the predominant texture. The increased cooling rate close to the part surface inhibited grain growth and changed the preferential grain orientation. For the process parameters used, the critical part thickness to avoid large elongated grains was found to be about 0.4 mm. The obtained results could be used for further development of design rules and prediction of mechanical properties of AM parts with small wall thicknesses.

Keywords: additive manufacturing, powder bed fusion, powder recycling, stainless steel, thin wall structures, microstructure, direct metal laser sintering, electron beam melting, 316L

Preface

The work has been carried out in the Department of Industrial and Materials Science, Chalmers University of Technology (Gothenburg, Sweden) under the supervision of Prof. Eduard Hryha and Prof. Lars Nyborg. This licentiate thesis comprises an introduction and a review of some aspects of powder bed fusion of stainless steel.

List of appendant papers

- I. **Degradation of stainless steel 316LN powder associated with additive manufacturing by Electron Beam Melting**
A. Leicht, R. Shvab, L. Nyborg, E. Hryha
Submitted
- II. **Surface Oxide State on Metal Powder and its Changes during Additive Manufacturing: an Overview**
E. Hryha, R. Shvab, H. Gruber, A. Leicht, L. Nyborg
Proceeding of Euro PM 2017 Congress & Exhibition, Milan, Italy 2017
- III. **Effect of build geometry on the microstructural development of 316L parts produced by additive manufacturing**
A. Leicht, U. Klement, E. Hryha
Submitted

Contribution to the appended papers

- I. The author planned and performed the experimental work, took part in the analysis of the results in collaboration with the co-authors as well as wrote the paper in close cooperation with the co-authors.
- II. The author performed the characterization and analysis of the stainless steel powder as well as participated in the writing of the paper.
- III. The author planned and performed the experimental work as well as the analysis in collaboration with the co-authors. The author wrote the paper in cooperation with the co-authors.

Paper not appended in this thesis

- I. **Characterization of virgin and recycled 316L powder used in additive manufacturing**
A. Leicht, R. Shvab, E. Hryha, L. Nyborg, L.-E. Rännar
Conference proceeding of SPS16, Lund, Sweden 2016
- II. **Characterization Of The Virgin And Re-cycled Nickel Alloy HX Powder Used For Selective Laser Melting**
R. Shvab, A. Leicht, E. Hryha, L. Nyborg
Conference proceeding of World PM 2016, Hamburg, Germany 2016
- III. **As-HIP Microstructure of EBM Fabricated Shell Components**
A. Leicht, M. Vattur Sundaram, E. Hryha, L. Nyborg, M. Ahlfors, L.-E. Rännar, K. Frisk
Conference proceeding of World PM 2016, Hamburg, Germany 2016

Contents

Chapter 1 – Introduction	1
1.1 Aim of the thesis	2
Chapter 2 – Metal Additive Manufacturing	3
2.1 Powder Bed Fusion	3
2.2 Process Cycle	5
2.2.1 Pre-processing	6
2.2.2 Building	6
2.2.4 Powder Recycling	7
2.3 Powder for powder bed fusion	8
2.3.1 Powder Characteristics	8
2.3.2 Powder Recycling	9
2.4 Stainless steel	10
2.5 Microstructure Development	11
2.6 Design guidelines and mechanical properties	14
2.6.1 Properties of PBF components	15
2.6.2 Design limitations	16
Chapter 3 - Experimental Methods	19
3.1 Material and sample preparation	19
3.2 Light Optical Microscopy (LOM)	20
3.3 Scanning Electron Microscopy (SEM)	20
3.3.1 Electron Backscattered Diffraction (EBSD)	21
3.4 X-ray Photoelectron Spectroscopy (XPS)	21
Chapter 4 - Results and Summary of Appended Papers	23
4.1 Powder degradation	23
4.2 Microstructure	25
Chapter 5 - Summary and Conclusions	27
Acknowledgements	29
References	31

Chapter 1 – Introduction

Additive manufacturing (AM) is defined by ASTM F2792-12a as “a process of joining materials to make objects from a 3D model data, usually layer upon layers” [1]. In the late 1980s, the process was used as a tool for making prototypes. At that time the process was immature and resulted in parts with quality that could satisfy only limited demands on mechanical properties, still enough for visualization and simple handling. Today AM has matured and can be used for fabrication of high-end fully functional parts besides its extended use for prototyping. The term additive manufacturing is very broad and covers a large number of different processes and materials, from consumer machines for 200€ up to high-end machines with a price well over million euro. Hence, parts can be made for a wide range of applications, including metallic materials like stainless steel, Ni-based superalloys, Ti- and Al-alloys, etc. The society has so far gained various benefits from the additive manufacturing industry, including customized healthcare products which have improved the wellbeing of the population, the raw material usage and energy consumption can also be reduced owing to potentially less scrap and hence more efficient material use, which is expected to contribute to sustainable development, etc. The AM market is growing fast with different stakeholders including process equipment manufacturers, software and material suppliers, subcontractors, etc. New value chains, business opportunities and business models are created thanks to the additive manufacturing during last two decades.

The AM supports the realization of advanced geometrical designs without extensive tooling as well as designs that would be impossible to create with conventional methods. The high degree of design freedom makes it possible to add functions without an increase in production costs. Hence, AM is said to provide complexity for free. At the same time, the design freedom means that already at the beginning of the product development stage, considerable reduction in cost and time can be achieved. These attractive characteristics of AM rely on the improved quality, which has made it possible to fabricate functional prototypes in early stages. The consequence is that the design iteration becomes faster and cheaper.

Metal AM has been around since the mid-90s and as for AM of polymers, the product quality was relatively poor at the beginning, with defects, porosity and lack of fusion commonly observed. Nevertheless, extensive research and development have resulted in hardware and process development, resulting in the successful technology establishment and manufacturing of the components for the number of alloys, including Ti- and Al-alloys, Co-Cr alloys, Ni-base alloys, tool and stainless steels, etc., that are currently available on the market. This means that parts with properties comparable or better with those obtained with conventional methods like casting and/or forging can today be fabricated. However, despite these efforts, the metal AM process is not yet fully developed into its full potential as reproducibility, productivity, process stability, robustness, etc., are still limited.

One of the most common processes for manufacturing of metallic components through AM today is the powder bed fusion (PBF) which uses a fine gas-atomized metal powder as a raw material. The AM-specific demands with respect to size distribution, purity and powder properties mean that such powder is relatively expensive. This means that recycling of unmelted powder from the process is of crucial importance. It is well known that the powder properties affect part quality, e.g. relative density, surface roughness and mechanical properties. Despite the number of the papers published in the topic of powder recycling, there is no clear understanding of the powder degradation phenomena. At the same time, little or no consideration has been dedicated to how the surface chemistry of the powder is influenced by the process and what is the role of the powder surface chemistry in powder bed fusion.

The PBF process has shown great potential for producing high-quality parts in stainless steel. The laser-based variant is considered to be well-developed with good buildability and a greater number of qualified alloys, while also the electron-beam based process of stainless steel has presented good potential in recent research [2,3]. Nevertheless, no conclusive research has been reported on how the microstructure of 316L parts are affected by build geometries in detail even if design freedom is one of the large advantages with AM.

1.1 Aim of the thesis

This thesis aims to provide basic knowledge on processing of stainless steel powder utilizing powder bed fusion in order to ensure a robust production of stainless steel components with complex geometry. The work is focused on understanding the fundamental link between feedstock material, AM processes, build geometries and their effect on the part quality. This will ensure high-quality parts realization with high degree of design freedom.

Chapter 2 – Metal Additive Manufacturing

This chapter will introduce the powder bed fusion process. Followed by a general explanation of the production cycle, the correlation between the process, microstructure and feedstock materials will be elaborated. This chapter facilitates a better understanding of how high part quality like density, surface roughness and mechanical properties, can be achieved through powder bed fusion.

2.1 Powder Bed Fusion

The AM technology enables the creation of near-net-shaped parts of almost all sizes and from all material groups. ISO/ASTM 52900 categorizes additive manufacturing into seven process categories: binder jetting, directed energy deposition, material extrusion, material jetting, powder bed fusion, sheet lamination and vat photopolymerization. When it comes to the metals, binder jetting, directed energy deposition, sheet lamination and powder bed fusion can be utilized. As mentioned in the introduction, the most common sub-technology for fabrication of metal parts is the PBF. **Fig. 1** illustrates a schematic overview of the two most common PBF setups with some of the most important system parts. Slight variations between different machine brands and processes will, of course, be the case.

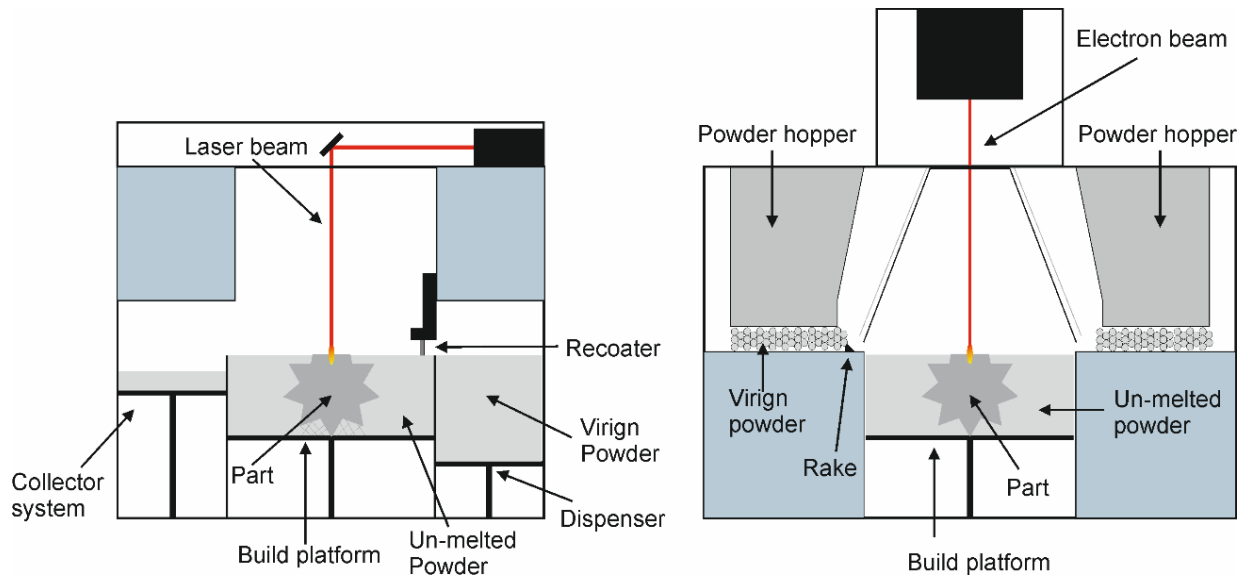


Figure 1: A schematic overview of an laser beam melting process (left) and electron beam melting process (right)

A common statement is that by utilizing AM and PBF, complexity can be added for free. This is especially true when comparing the PBF technology with conventional methods, like casting, forging, etc., see **Fig. 2a**. Traditionally the cost is continuously increasing with increased complexity. However, by means of PBF the part cost is more or less constant

regardless of complexity and is determined only by the volume of the part. Still, the PBF technology has some limitations when compared to other powder metallurgy (PM) processes, also utilizing powder as the base material, such as hot isostatic pressing (HIP), metal injection molding (MIM) and classical “press and sinter”; as shown in **Fig. 2b and c**, PBF means restrictions in both production volume and part sizes. The production volume is limited by the relatively small build area/volume and slow building time. As an estimation, a few cm³/h can be fabricated, which is magnitudes lower than what can be achieved by e.g. “press and sinter”. The part size is limited by the size of building chamber, usually about 25x25x30 cm, but also by the part size since large parts will increase the process time significantly. By employing AM, material is only added where needed which opens up the possibility to create lightweight structures as e.g. lattice designs, with minimum machining which also causes high material utilization. Since the design freedom is very high, new functions can be created which would have been impossible to make with conventional methods as e.g. complex internal cooling channels. This types of features have been fabricated by PBF for e.g. the polymer injection moulding industry, where moulds have been fabricated. Due to the unique design possibilities by AM, the cooling channels were optimized for maximum heat conduction, which resulted in higher productivity and extended tool life [4,5].

Further challenges with PBF is the limited numbers of materials available. At the current state of the art, there are only about 12 alloys publically available, that are typically weldable materials. In most cases, the parts fabricated by PBF will show anisotropy with different mechanical properties along and across the building direction, even if the mechanical properties, in general, are comparable with wrought materials and better than casting. Another challenge is the pre- and post-processing. In post-processing, support structures needed at overhangs must be removed from the final product. Additionally, surface finishing and heat treatment may be required.

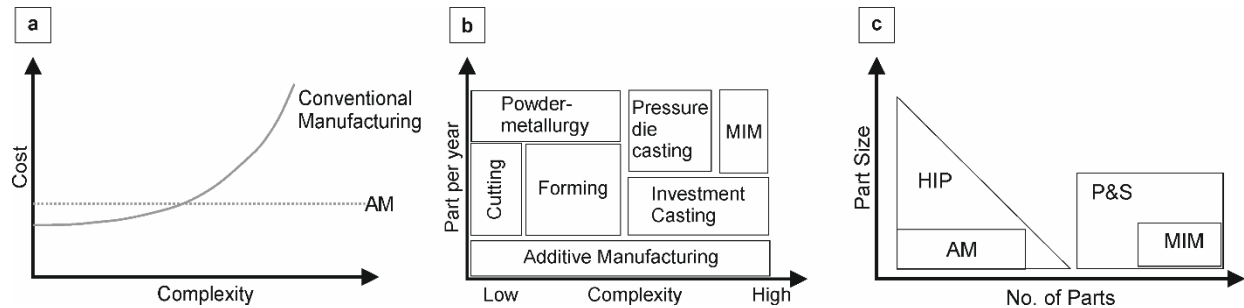


Figure 2: Illustration comparing AM to other technologies; (a) the correlation between part complexity and cost for conventional manufacturing and additive manufacturing (b) the production volume and complexity for different PM technologies (c) the possible production volumes and part sizes for different PM technologies.

The foremost important PBF systems can be divided into two different processes depending on the heat source: laser beam melting (LBM) and the electron beam melting (EBM). Binder jetting also belongs to PBF systems but will be overlooked in this thesis. The LBM process involves the use of a high-quality laser beam, typically from an Nd:YAG source. The beam is guided by mechanically movable mirrors onto the powder bed as shown in **Fig. 3a**. The movement of mirrors has a physical limitation when it comes to the speed that, hence, limits

the build speed. The process is performed at slightly elevated temperatures, typically between 60 and 200°C, and the build chamber is filled with an inert gas, commonly argon or nitrogen, in order to minimize oxidation of both powder and the fabricated part. The LBM process requires powder in the range from 10 to 60 μm , depending on the hardware.

In the EBM process, a high energy electron beam with high melting capacity will be generated from a hot tungsten filament or a LaB_6 filament. As shown in **Fig. 3b**, the beam is controlled by electromagnetic lenses which makes the process and scanning of the beam faster and more accurate than in case of laser-based systems. This increases the productivity as compared to the LBM systems. However, the use of electrons means that the process must be run in vacuum and the powder bed needs to be conductive. To increase the conductivity and to avoid sputter of over-charged metal particles, each powder bed layer is pre-sintered and preheated to a material specific temperature. The pre-sintering will slightly sinter the powder bed creating a “cake” of powder, which provides natural support for the build components. This powder cake needs to be crushed when the build is finalized in order to recycle powder. The preheating temperature is kept throughout the build forming an in-situ stress relieving that reduces the thermal stresses significantly. In case of the LBM systems, the thermal stresses in the part are so high that shape distortion may occur if the stresses are not released before removal. The EBM process requires somewhat larger metal particles, usually 50-150 μm compared to the typical range used for LBM (10-60 μm). The main reason is to avoid over-charging of the powder by the electron beam. The use of coarser powder results in a rougher surface on the part built with EBM compared with LBM.

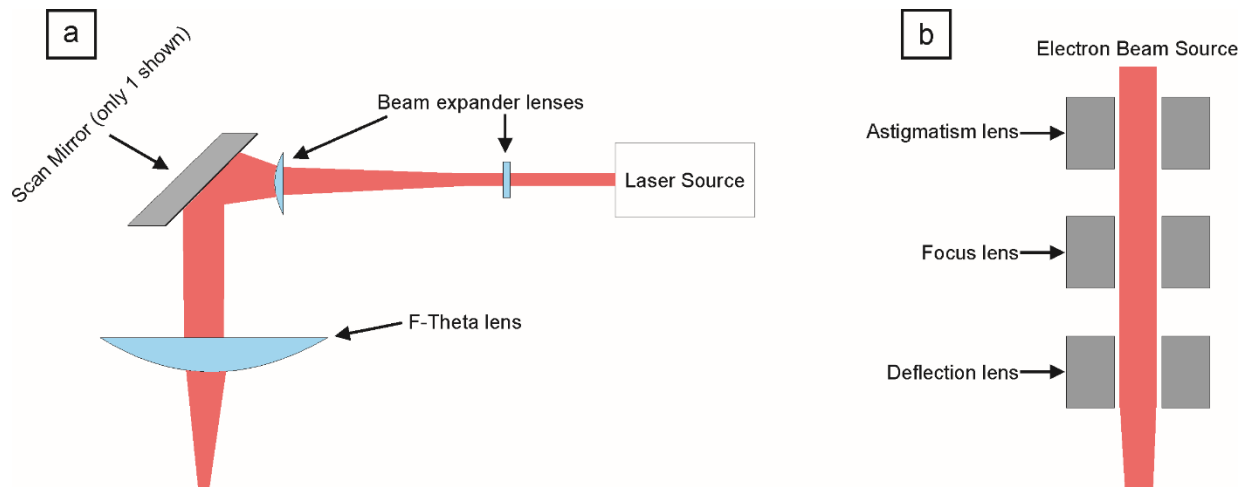


Figure 3: A schematic overview of the beam control in (a) LBM and (b) EBM.

2.2 Process Cycle

In order to create a robust manufacturing routine, the whole processing chain from raw material to the final part needs to be controlled. In this section, a general description of the basic procedures of a PBF process will be presented. The procedures are similar for both the LBM and EBM technologies, but important differences will be addressed.

2.2.1 Pre-processing

Initially, the parts need to be created using a 3D CAD-program, involving that the model is converted to an STL format. The strength of the STL format is that it was primarily developed for AM and is a standard in the AM industry [6]. Since all CAD software will represent the part in different ways, the conversion to SLT creates consistency. The STL format is based on a triangular representation of the part and for this reason, no exact representation of curved features, etc., can be presented but by increasing the number of triangles a good approximation can be accomplished. The STL file is imported to a special software where the build orientation is defined and support structures are added. The STL is thereafter sliced into thin cross-sectional layers and together with process parameters and a set of files is transferred to the PBF machine where the support structures and part are created by selectively consolidating the powder in a layer-by-layer manner until the part is finalized.

2.2.2 Building

The build initiates by applying a thin powder layer on a build plate with 20-50 μm thickness for the LBM process and 50-100 μm thickness for the EBM process. The beam will be directed onto the powder bed and selectively melt the powder by creating a melt pool through the heat absorption by the powder. The size of the generated melt pool is determined by the size of focus of the energy source and scanning speed and is typically between 50 and 300 μm , larger in case of EBM. In case of the EBM process, prior to melting the powder bed is preheated by means of special fast scanning of the electron beam, while pre-heating in this manner is not possible for LBM. In either case, for the main building, as the beam moves away from the melt pool generated, the rapid solidification starts. The cooling and hence solidification are fast; local cooling rates in PBF in the rage of 10^5 - 10^7 K/s are expected [7]. The building is controlled by a set of processing parameters like layer thickness, hatch distance, spot size, focus, power, scanning strategy, etc. The most common scanning strategies are stripe pattern or island patterns as shown in **Fig. 4**. In case of the stripe, the scan direction is rotated 67° in each layer, see **Fig. 5**. The different scanning strategies and processing parameters will strongly influence the final quality, i.e. defect, microstructure, surface roughness and residual stresses. To ensure that the high-quality parts will be created, optimized process parameters are necessary. When the melting is completed, the build plate is lowered and the cycle is repeated until the part is finalized.

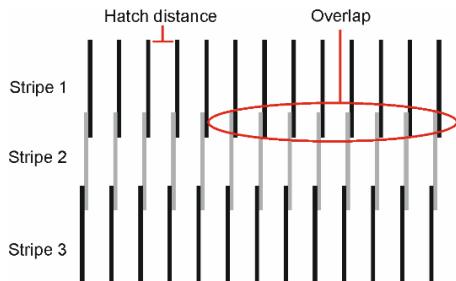


Figure 4: Two common scanning strategies used in PBF: (a) stripe pattern and (b) island pattern.

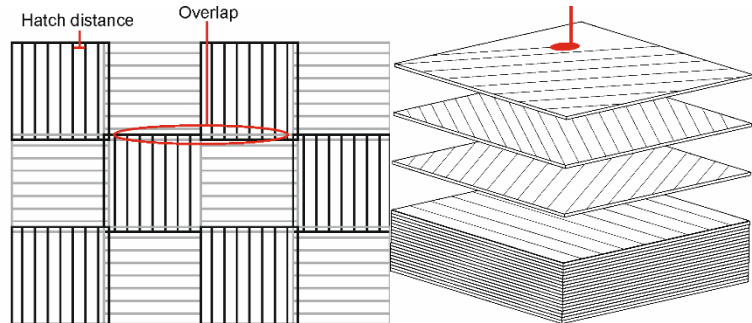


Figure 5: Rotation of scan direction.

2.2.3 Post-Processing

It has been estimated that up to 70% of the part cost may be assigned to the pre- and post-processing. Consequently, this is a major concern for the AM industry at the current state-of-the-art. The post-processing is usually done manually and involves removing the un-melted powder, detaching the part from the build plate and removal of the support structures. Depending on application, heat treatments such as tempering, solution annealing, stress relief and hot isostatic pressing (HIP) may be required, which would increase the total production costs. Furthermore, the PBF process is associated with rough surfaces which in many cases requires abrasive finishing like blasting and polishing.

2.2.4 Powder Recycling

PBF is associated with a high material utilization and thereby good economic feasibility for high price materials. To facilitate this, the un-melted powder after each build needs to be collected and recycled. The following procedures are performed in a recycling sequence: prior to the build, the machine is loaded with fresh powder, so-called virgin powder, which will be used for the first build when the part is finalized. The un-melted powder in the build volume and in the collector bin is vacuumed and sieved to maintain the original size range. The sieved powder is mixed with a fraction of virgin powder creating a blend which is used for the next build. A schematic overview of the sequence can be seen in **Fig. 6**. The procedure of the powder recycling is dependent on the material and hardware utilized and is not regulated by any standards and therefore is based on the “best user experience”. Therefore, very little information is available on how the recycling should be performed, e.g. how many times the powder can be recycled and how large fraction of recycled powder that should be mixed with fresh powder, etc. There is also a difference between the EBM and the LBM processes when it comes to powder recycling. Since the EBM process involves pre-heating each powder layer, a sintered cake of powder will be created. This cake will be kept at the pre-heating temperature through the whole build time which in many cases is several hours. In LBM, the powder in the bed is only heat affected by the built part and if the build plate preheating temperature, if applied, which is significantly lower than in EBM. The effect of recycling on the powder will be elaborated in more detail in section 2.3.2.

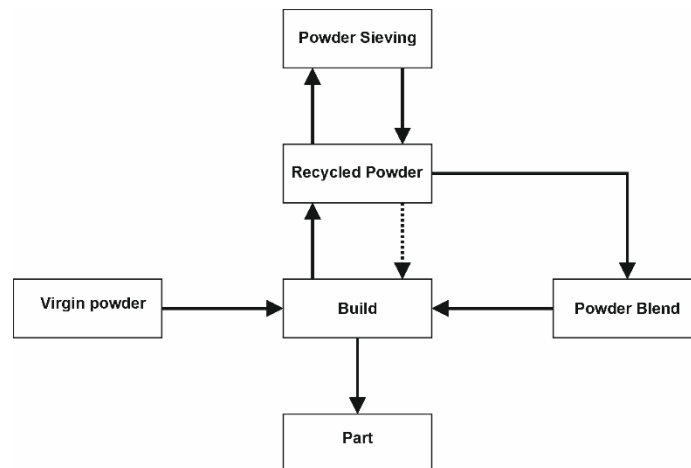


Figure 6: Overview of the recycling cycle.

2.3 Powder for powder bed fusion

Most of the commercially available powder for AM is produced by gas atomization, in which a high-pressure gas stream breaks the molten metal and produces droplets which solidify into spherical metal particles in a wide array of sizes. Most of the powder used in AM is produced by either Electrode Induction melting Gas Atomization (EIGA) or Vacuum Induction Gas Atomization (VIGA). When manufacturing powder of alloys that are sensitive to oxidation, like stainless steel, an inert gas is chosen as atomizing medium, usually argon or nitrogen. The processes are associated with low productivity and high price. However, the produced powder will have high sphericity with, typically, a clean and smooth surface and a low amount of satellites, see **Fig. 7**. These types of powder characteristics are desired when it comes to producing high-quality parts by PBF [8–12]. The produced powder will have a large size range (1-150 μm). Therefore, the produced powder is sieved and mixed to create a batch with wanted powder size distributions (PSD). Hence, the prices will to some extent be determined which PSD that is used.

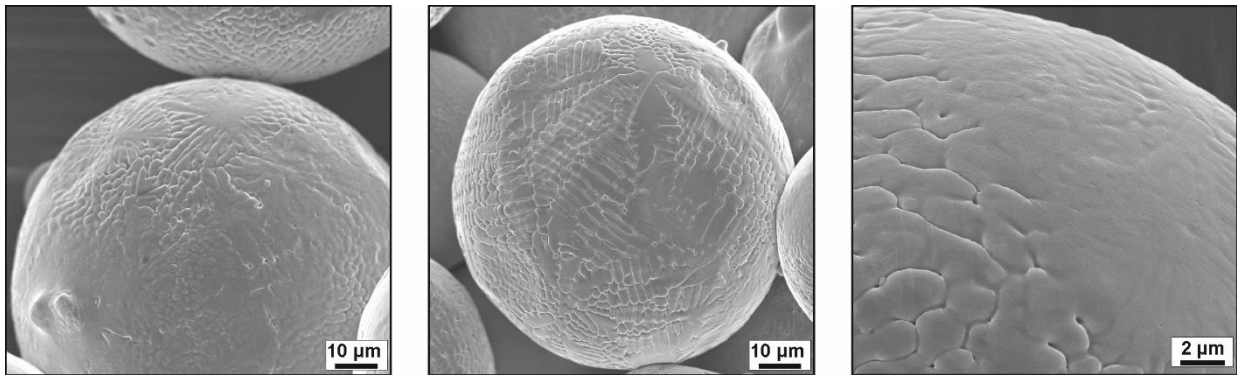


Figure 7: SEM image showing gas atomized 316L powder particles produced by VIGA.

2.3.1 Powder Characteristics

From the ASTM F3049-14 the following powder characteristics can be identified: size distribution, morphology, chemical composition, flowability and apparent density. These characteristics comprise a mixture of measures based on both theory-based and empirical methods. Understanding the effect of these characteristics on final built part quality is fundamental for further development and improvement of the AM technology. The characteristics are supposed to represent the powder quality and it is expected that the powder quality may influence several important aspects of the PBF process, including the achievable mechanical properties, defect formation, reproducibility, build consistency, etc. A broad explanation of how each of the powder characteristics will affect the process and its implication on part quality will be described in this section.

An important powder characteristic for the PBF process is flowability (how well a powder flows). Poor flowability could lead to inhomogeneous spreading and low packing density. The packing density is a measure of the capacity of powder to gain certain relative density and it will be affected by the flowability, which in turn is determined by the inter-particle friction. At low powder bed density, defects like lack of fusion and porosity will be more easily generated. Therefore, to fabricate defect free parts with good dimensional accuracy, the powder should have as high flowability as possible [8,13–15]. However, to ensure both high

flowability and high packing density, powder PSD needs to be optimized. The PSD should be intermediate since wide PSD will reduce the flowability whereas a narrow PSD could lead to insufficient packing density [8,14–16]. The flowability is also affected by the powder morphology; irregular powder and large amount of satellites will decrease flowability, whereas small spherical particles with smooth surface promote better flow [13–22]. Moreover, the powder itself needs to be defect-free since internal porosity increases the risk for defects like gas porosity and lack of fusion in the final product [20].

Parts produced from powder will be strongly affected by both the surface chemical composition and the bulk chemical composition of the feedstock. It is therefore essential to understand how the powder surface chemistry affects the part quality. However, so far little attention has been dedicated to this topic. Nevertheless, some studies have shown that to avoid defects, like balling and lack of fusion, good wetting to the underlying substrate is vital. Surface contamination and/or presence of surface oxides means that the wetting might be reduced and hence the risk for defects increases [23]. Therefore, the powder should be handled with care both inside and outside the process. To avoid oxidation of the powder inside the build chamber, where it is exposed to an elevated temperature, an inert gas or a high vacuum is needed to protect the powder surface. This is especially important for the materials which are alloyed with elements sensitive to oxygen, like stainless steel, Ti, and Al-alloys [14,23–25]. The large surface area of the powder in combination with the presence of elements with high oxygen affinity, like e.g. Cr, Mn, Si, Ti, Al, etc., can result in significant oxidation of the powder which could affect the particle bonding to the layer beneath and hence impact the quality of the part [26]. Finer powder will tend to have higher oxygen content due to the higher specific surface area compared to that of the coarser powder. The chemical composition also will influence many material characteristics like melting temperature, mechanical properties, thermal conductivity, heat capacity, etc.

2.3.2 Powder Recycling

The powder recycling, explained in section 2.2.4, can affect several of the powder characteristics mentioned before like chemical composition, surface morphology (surface roughness, particle roundness), physical properties (flowability, PSD, etc.). In this section, some of the key findings in literature will be discussed in terms of implications for robustness of the process. Several studies have been conducted on the effect of the powder recycling on the change in the powder bulk composition, particle size, apparent density, tap density, particle morphology and particle size distribution, etc. Most of the studies have been directed on Ti-6Al-4V or Ni-based alloys. Most of the recyclability studies that have been conducted indicate that the EBM process affects the powder more than expected, due to the pre-sintering as well as exposure of the powder cake to rather large temperature for long build times [20,27–30]. However, different alloys will be affected in different ways. For example, Ti-6Al-4V will create a stable oxide layer as well as dissolve some oxygen in the matrix compared to high-alloyed steels as e.g. 316L that will create particulates on the surface instead.

When the powder is recycled, slight oxygen pick-up can be expected from atmospheric exposure, especially during the blasting and sieving steps. Also, the time and temperature that the powder experience in the AM process might lead to thermally activated oxide growth on the powder surface and hence powder degradation. If the powder is recycled for number of

times (over 30 cycles) morphology change of the powder particles can be expected [10]. A slight increase in powder agglomeration can be expected, which may result in change in powder sizes and narrower PSD. In general, for both LBM and EBM, the powder becomes more irregular and the surface becomes rougher after recycling [30–32]. An unexpected result was that the slightly better flowability was shown after the recycling, but with some decrease in the tap density. It was proposed that it is connected to the moisture loss upon AM processing due to the heat in the process [30]. A drier powder will, in general, have better flowability [10,33,34]. Still, even if changes in powder characteristics have been shown when comparing recycled and virgin powder, no significant differences in mechanical properties between parts built without and with re-cycled powder has been proven [20,30].

To summarize, the flowability seems to be the most important factor that is affecting the AM product quality. The flowability is expected to be related to resistance in moving between particles, determined by the surface area, surface roughness and surface chemistry. There are, of course, many more powder-specific factors that will affect the part quality, but ensuring high layer density with high evenness is a critical aspect. To achieve this, both the process and the powder characteristics need to be well understood. From the short review above, it is clear that recycling process affects the powder properties. Therefore, it is crucial to further investigate how different AM processes affect the powder and the impact on part quality. It can also be concluded that more attention to powder recycling is needed when using the EBM process than when the LBM process is used.

2.4 Stainless steel

Stainless steel has been used as an engineering material for decades because of the combination of good mechanical properties and excellent corrosion resistance. This combination has made the material suitable for a wide range of applications in several different sectors such as gas and oil, chemical and petrochemical, marine engineering, food preparation, pharmaceutical and medical parts.

One of the most common alloys used in PBF is the stainless steel 316L. The alloy is a fully austenitic material which for the cooling rates of concern does not undergo any phase transformation upon cooling. The material is also considered to be fairly stable. To stabilize the austenite and ensure corrosion resistance, both Cr and Ni are added [35]. To ensure that the steel is stainless, at least 12 wt.% of Cr needs to be contained in the alloy to create the protective oxide layer that will give both oxidation and corrosion resistance. Nickel needs to be at a sufficient level so that the austenite phase can be retained up to the melting temperature. Moreover, low amount of carbon will limit the risk for formation of Cr-rich carbides. These carbides would reduce the local corrosion resistance drastically and lead to intergranular corrossions. Also, the cooling rates of concern in PBF (10^5 - 10^7 K/s) means that sigma phase formation is not viable. The facts amongst others means that single austenitic phase structure is expected, which makes the 316L suitable for PBF.

2.5 Microstructure Development

The properties and quality of a metallic part will, to large extents, be determined by the microstructure and the amount of defects. The following sections will elaborate on the development of the microstructure in the component fabricated by means of PBF with the particular reference to austenitic stainless steel.

The typical PBF microstructure is formed by a complex thermal history with several process characteristics. Understanding these characteristics is crucial when developing the PBF process, for new materials or performing process parameters optimization. The thermal history will depend on the AM process type, metallurgy of material used and process parameters. Therefore, a diversity of microstructures can be formed [36–38]. Consequently, it is difficult to make a universal assumption regarding the solidification structure and its appearance. Nevertheless, some facts can be stated regarding the microstructure. Stainless steel parts fabricated with PBF will have microstructure characterized by melt pool boundaries, laser scan tracks and large columnar grains with a fine cellular structure and precipitates in the cells boundaries.

The melting process initiates when the beam, with a small spot size (100-150 μm), interacts with the powder bed and by radiation heats the powder well above the melting point, forming a pool of liquid metal. Both the heating and cooling rates are extremely high owing to the small interaction volume and solidification starts as soon as the laser beam moves away. To ensure a fully consolidated part without large defects or lack of fusion, the beam is set to penetrate 3-5 layers down into the powder bed and therefore fully or partially re-melt the already solidified layers below. This is schematically shown in **Fig. 8**. The rapid heating and cooling followed by the re-melting will generate high internal stresses (by the constraining surrounding material) and thermally affect diffusional processes like grain growth, phase transformations and precipitation, resulting in a non-equilibrium microstructure [39–43].

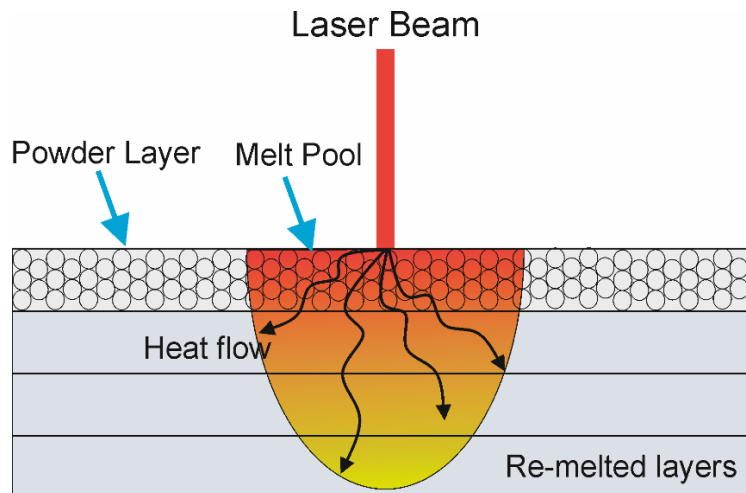


Figure 8: Schematic view of the melt pool and the partial re-melting which creates a heat flow.

This procedure will generate a microstructure consisting of several melt pool boundaries as seen in **Fig. 9**. The size of a melt pool is commonly 100-200 μm in width and 25-100 μm in depth. The depth of the melt pool is an indication of the penetration and re-melting while the distance from center-to-center is an indication of the hatch distance. Furthermore, as can be seen in **Fig. 10**, the microstructure consists of large columnar grains that are aligned in the building direction. The grains stretch over 100 μm and hence cover several build layers. There is no tendency for the melt pool boundaries to affect the grain direction. This type of crystallographic orientated grain structure is commonly associated with AM parts of most metallic materials [36–38,40,42–48]. The melt will solidify and keep the same crystallographic orientation as the previous grains as they are nucleated from and grow in the direction of the maximal thermal gradient in an epitaxial manner [48].

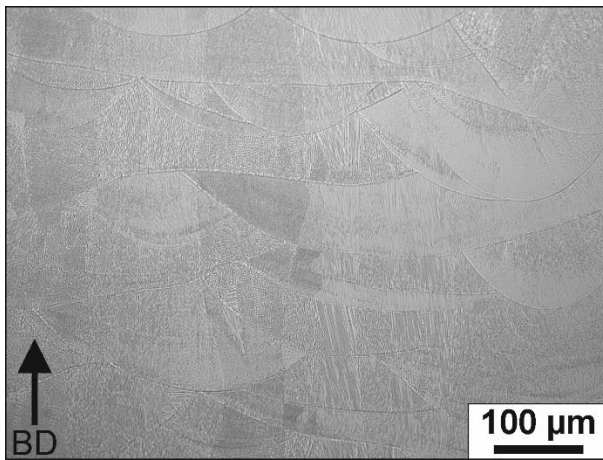


Figure 9: SEM micrograph showing several melt pool boundaries

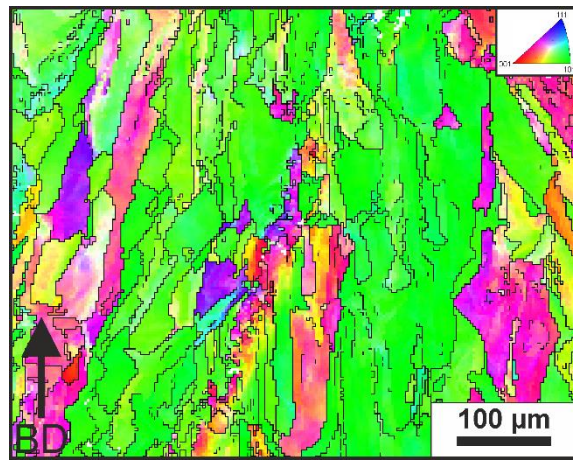


Figure 10: EBSD maps showing IPF coloring in the building direction with high angle grain boundary (black lines)

The development of the microstructure will be determined by the temperature gradient (G) and the growth rate (R) at the solidification interface (between solid and liquid) [7,39,45]. The product $G R$ represents to overall cooling rate. The solidification mode may change from planar to cellular, cellular-dendritic or dendritic depending on the undercooling [7,45] as schematically shown in **Fig. 11**. The solidification mode will also be determined by the ratio between the gradient and the growth rate. High G/R ratio will generate a planar mode while a low G/R will generate dendritic solidification. The cellular structures observed in PBF indicate an intermediate G/R . Furthermore, the cooling rate given by the product $G R$ will control the spacing between the microstructure constituents. Since very high cooling rates have been reported (10^5 - 10^7 K/s), fine cellular morphology is formed [7,45]. The growth of the cellular structure (frequently referred to as sub-cells) is controlled by the advancement of the solidification front which in turn is controlled by the thermal gradient. Higher heat transfer results in finer cell structure while the slower dispersion of heat gives coarser cell structure [7,39,45].

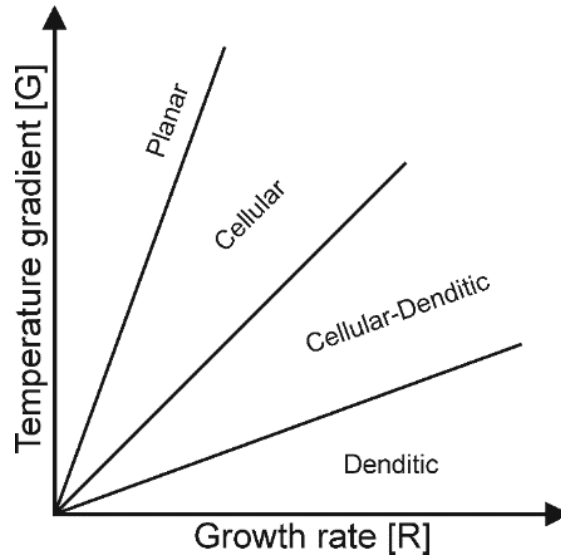


Figure 11: Schematic overview of the effect of temperature gradient and growth rate on the different solidification modes

This fine cellular structure can be observed at higher magnification as shown in **Fig. 12**. The size of the cells is generally of between 0.5-1.0 μm in diameter and length reaching 10 to 100 μm . The cells are elongated and can have different growth directions as can be seen by comparing **Fig. 12a and b**. The observed alteration in growth direction may originate from a local change in temperature gradient inside the melt pool [43,45,48,49]. Comparing with microstructures produced by manufacturing techniques that traditionally have been considered to include fast cooling such as welding, the microstructure obtained in PBF is much finer and unique in comparison with microstructures obtained by other metal forming processes [37,48]. By changing the processing parameters as e.g. energy density, alteration of cell/dendrites sizes can be achieved owing to the different thermal history. By using higher energy density, higher thermal input leads to coarsening of the cells [7].

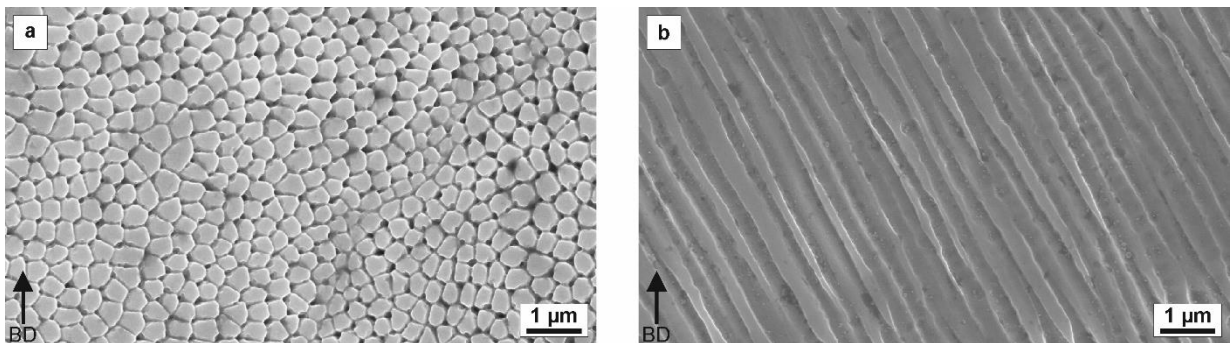


Figure 12: SEM micrograph showing a fine sub-cell structure in two different orientations (a) perpendicular to the building direction and (b) parallel to the building direction.

The cells are separated by the cell boundaries. In case of **Fig. 12** they are not visible as this sample has been electro-chemically etched in oxalic acid which will preferentially attack the cellular boundaries. Studies by Z. Sun et al. and Y. Zhong et al. have shown that cell

boundaries have higher Mo content and higher dislocations density [37,43]. Hence, an intergranular cellular segregation network is formed [43]. Similar segregation has been reported for casting of 316L, the difference is that the cooling rates are much higher in PBF which will result in finer microstructures. It is reasonable to assume that the high dislocation density is generated by the rapid cooling associated with the process. It has also been reported that nano-sized inclusions, rich in Si, are found close to the cell boundaries. Hence, by having a high amount of oxygen in the build chamber, more inclusions could be formed. Such inclusions could potentially increase the mechanical properties by hindering dislocation movement [37,43,49,50].

Initial studies have been done to fabricate 316L by means of EBM [3,51]. In general, high density was achieved (99.8%), but a few large pores were observed which was believed to be the result of non-optimal process parameters, as e.g. to thick powder layers [3]. The microstructure is similar to what has been observed for LBM samples, but with different characteristics regarding the cell structure. By means of energy-dispersive X-ray spectroscopy (EDX) analyses, precipitates containing more Cr and Mo were found at the grain boundaries which were not as easily observed in LBM samples. However, no sigma or laves phase was found. This might be caused by the fact that the part is kept at elevated temperature during the whole built by the electron beam pre-heating approach and possibly cooling conditions associated with the EBM process. It was argued that the precipitates might increase material brittleness and hence decrease mechanical properties. The geometry of the cell boundaries had a more irregular shape compared to what has been observed in the LBM samples. Again, the elevated temperature maintained for long time in EBM was believed to be the cause for these differences. The reason was supposed to be that the elevated temperature allows for more diffusion of any segregated elements from the sub-cell boundaries. Still, even if the EBM samples can be close to an annealed state, the microstructure was different from what has been observed from conventional 316L samples.

To summarize, parts fabricated with PBF will consist of anisotropic microstructure with large elongated grains oriented in the building direction. In some cases, these have preferential crystallographic orientation. Inside these large grains, a fine cell structure is created [45]. It is believed that the small size of the cells is a main reason for the improved mechanical properties for LBM-processed 316L compared to those for conventional wrought or cast 316L parts [38,52]. The fineness of the cell structure is supposed to be dependent on the cooling rate experienced in the PBF process.

2.6 Design guidelines and mechanical properties

The part quality depends on the mechanical properties which are profoundly determined by the microstructure and the amount of defects and in turn depend on the process parameters. Additionally, the part quality will be determined by design aspects affecting the thermal gradient in the parts such as build orientation, wall thickness, support structures, overhangs, etc. In this section, some of the key mechanical properties will be elaborated together with the design advantages and limitations of the PBF process.

2.6.1 Properties of PBF components

It is well established that even if PBF parts are characterized by an anisotropy in microstructure and hence properties, the yield strength for the weakest direction has been demonstrated to be comparable to that obtained with conventional methods like forging or casting, in case of well-established PBF process. In PBF of stainless steels, the lowest strength and ductility are achieved in a vertically built tensile specimen, see **Fig. 13**. Despite of the comparably high strength, there are still some challenge with the elongation to fracture shown to be inferior in AM parts compared to that of its wrought counterparts [7,38,42,48,49,53,54]. As mentioned in section 2.5, the microstructure consists of large elongated grains with a fine cell structure inside. As long as the density is high (over 98%) the main features that will contribute to the tensile strength are the three kinds of boundaries: melt pool boundaries, grain boundaries and the cell boundaries. It is assumed that the cell boundaries are the most significant characteristic governing the properties. The cells are supposed to accumulate dislocations at the boundaries and hence this is expected to generate a positive effect on the tensile strength [7,38,43,55]. Of course, weak cohesion between powder layers could occur even with a high density, which would have a negative impact on the properties.

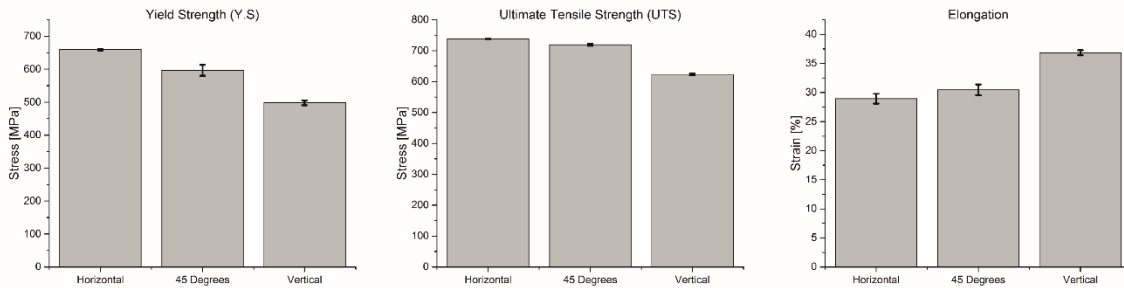


Figure 13: Tensile properties in different build orientations [56]

The most common defects created in PBF parts are pores obtained during the PBF process as well as pores arising because of gas entrapped inside the powder during the powder fabrication. Defects are undesired due to their tendency to weaken the materials and generate spread in the mechanical properties like e.g. ductility [43,48]. Pores in PBF are typically filled with argon that cannot be dissolved in the metal and hence the gas will remain as porosity. Consequently, pores filled with argon cannot be healed by subsequent hot isostatic pressing. Other defects that could be found in PBF parts are lack of fusion, cracks and un-melted particles. The defects are commonly created in the interface between layers. Hence, by having high number of layers would increase the risk for defects [7,35,57]. Therefore, by having a part oriented normal to the building direction compared to a parallel one, as seen in **Fig. 14**, improved final part properties can be gained. Furthermore, since the grains are elongated in the building direction, having the part orientation normal to the building direction may minimize microstructure anisotropy and improve the mechanical properties further.

The surface roughness will affect both the mechanical properties (especially fatigue properties) and the appearance of the manufactured part. A poor surface quality will need to

be post-processed and complex shaped parts might need to be manually treated. Hence, to ensure a good yield from the PBF, the required surface quality needs to be considered. The surface quality will be determined by the powder size, layer thickness, processing parameters as well as the orientation of the build surface in the build chamber. The surface will have some slightly sintered metal particles, as can be seen in **Fig. 15**. Thus, the metal particle size will affect the surface roughness [58]. Parts produced by means of EBM will generate poorer surface finish compared with LBM, the reasons being the use of larger powder in the former case and, in general, the thicker layers. The layer thickness affects both the production rate and the surface finish. Hence, increasing the production rate decreases the surface finish [59]. Furthermore, it has been shown that by the re-melting and applying contour scanning, the surfaces can be improved. However, this will also result in lower productivity [41,60]. Other processing parameters that will affect the surface roughness are hatch distance, power and scan speed as well as material properties [61]. To improve the surface finish, post-processing is applied. Amongst others, methods applied include electropolishing, sand blasting, grinding, etc. However, the surfaces need to be accessible to make it possible to be processed. Hence, finer internal structures as e.g. small internal cooling channels, are problematic to treat with traditional post-processing, bringing some limitation to the design freedom.

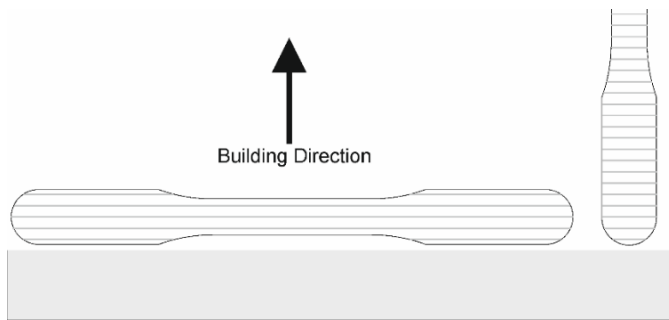


Figure 14: Part orientation effect on the number of layers.

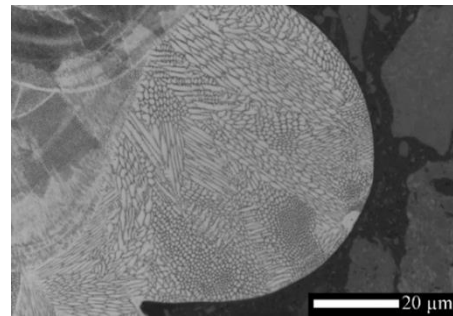


Figure 15: Sintered metal particle on the surface of a PBF part [62].

2.6.2 Design limitations

In this section, some of the design guidelines associated with PBF will be elaborated and connected to the quality attributes such as surface roughness, mechanical properties, density, residual stresses and dimensional accuracy. In order to generate good quality and a feasible economy, demands are put on proper design for AM and especially its connection to the post-processing, depending on the requirements on the component and its surfaces characteristics. It could be argued that robustness of the PBF process is limited by part accuracy, surface finish, repeatability and the restrictions in material selection. Elaborating and highlighting these limitations could further strengthen the application of the PBF process. Therefore, establishing sets of design guidelines could improve the use of PBF and result in further improved products. However, the design guidelines must also emphasize the limitations of the PBF process, rather than provide design features as e.g. maximum build angles, minimum wall thicknesses, etc. Addressing how these limitations affects the part quality, can then increase the robustness of the PBF process by allowing design choices based on function, appearance and quality. It is also important to mention that the current design limitations are hardware-dependent and they are also continuously altered and processing technology is developed and hence has to be periodically reconsidered.

First of all, in order to achieve repeatability for fabricated parts, good control of the process and the process parameters are a must. Hence, well-established process parameters are required as well as a well-controlled feedstock material. Failure to properly design components for AM will bring significant risk of either underperforming components or decreased economic feasibility/increased component price. Furthermore, the improper design (improper component orientation or support structures, etc.) significantly increase the risk of the build failure due to the limitations of the hardware. However, as mentioned before, adding complexity is a superior way for increasing value of the AM process. Therefore, an overview of some of the geometrical elements that need to be addressed for a successful and high accuracy build will be discussed. However, there might be constraints that differ between processes and hardware as the powder spreading (different blade materials as HLS-steel, ceramic, carbon brush, rubber rake, etc.), scanning strategy, etc. These differences will generate different constraints. Nevertheless, some general rules can be provided.

An important design feature for the PBF process is the possibility to make struts and lattice structures which can be used for fabricating light-weight components. A number of generic design criteria has been developed as follows. By making the wall and struts as thin as possible, the weight of the component can be reduced. The struts can be made down to a diameter of 0.15 mm while walls have a minimum thickness of around 0.2 mm [63]. However, a thin wall might not be self-supported meaning that when the rake spreads the powder failure might occur. Furthermore, most processes have a limitation in the length-to-height ratio which in most cases needs to be below 8:1. The designs are, of course, not always straightforward meaning that the part will be built at an angle. This will create an overhang with a top surface and a bottom surface, commonly known as top-skin and bottom-skin. The recommendation is that build angles lower than 45° should be supported from below. It has been shown that by decreasing the build angle the staircase effect increases and also the surface roughness [64]. Since the process is done in a layer-by-layer manner, a layer thickness will generate a stair height and the staircase effect is the approximation of a single layer compared to the CAD model, see **Fig. 16**.

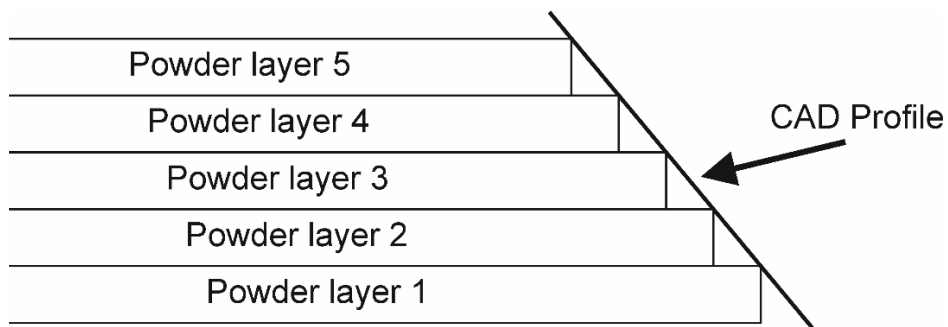


Figure 16: The staircase effect created by the PBF process due to the layer-by-layer processing

Another potential application is the fabrication of tools with internal cooling channels which has shown to be a promising business case. To fabricate these channels, holes of different diameters are needed with a recommended minimum diameter of 0.4 mm. The main problem with these small holes is the powder removal, especially if the cooling channels have a

complex pass. The beam intensity has to be carefully adjusted to avoid too deep penetration into the powder bed and hence risking that the walls of the fine channels are fused together. In the upper range, holes over 10 mm in diameter will need support structures. These supports need to be removed which could be difficult in e.g. internal cooling channels. However, by a proper design, the need for support structures might be eliminated; for example, by making the channels like keyholes or more oval in cross-section. Furthermore, in general, when making channels, subsequent surface treatment will be challenging since the channel is more or less impossible to access with any tools. There are some methods that involve etching with fluids or utilization of the abrasive liquids at elevated pressures, etc. However, these are in many cases both expensive and time consuming.

The support structures have several functions including supporting of overhangs, conduction of heat, prevention of warping, etc. At the same time, the support structures should also be easy to remove and should be minimized in number and complexity. By proper part design and orientation on the building platform, the amount of the support can be reduced or placed so that their removal becomes easy. The build surface supported will almost always need some kind of post-AM finishing. The part orientation will influence both quantities of support and the build time. Optimizing the built orientation could reduce the build time by e.g. lowering the part height and hence reducing the number of layers that need to be spread, which would reduce the cost significantly.

Chapter 3 - Experimental Methods

3.1 Material and sample preparation

In this work, sample fabricated from two different additive manufacturing processes (LBM and EBM) have been used for investigation. Both processes utilized a gas atomized stainless steel powder as feedstock, with specific grade and particle size distribution (PSD) for each process. The LBM process utilized a 316L powder grade with a PSD of 25-53 μm , whereas the EBM process used 316LN powder grade with a PSD of 53-150 μm . The measured chemical composition of each powder can be seen in Table 1. The 316L grade has a lower amount of carbon as compared to the normal 316 grade while the 316LN grade combines lower carbon content with higher nitrogen content to increase the high-temperature resistance.

The paper I and II covers the powder characterization with focus on recyclability and degradation of the powders materials. The powder in paper I was processed in the Arcam A2 EBM machine at Mid Sweden University, Sweden, while the powder in paper II was processed in the EOS M290 machine at Chalmers University of Technology. In paper III, characterization of 316L parts produced with the EOS M290 process is presented. All the parts and powder grades investigated have been processed with the standard process parameters provided by the machine manufactures and the solid parts were investigated in as-built condition.

Table 1: Chemical Composition of the powder grades used

Elements	316L [wt.%]	316LN [wt.%]
Fe	Bal.	Bal.
C	0.00939	0.0183
Cr	17,4	17.6
Mn	1.6	1.7
Mo	2.7	2.5
N	0.0568	0.0948
Ni	13.4	12.4
O	0.0436	0.014
P	0.006	0.008
S	0.00526	0.0061
Si	0.3	0.47

All the solid samples, characterized in this study were prepared using standard metallographic procedure including cutting, grinding and polishing. The samples were sectioned either along the build direction creating a cross-section in Z-plane or cut perpendicular to the build direction creating a cross-section in the XY-plane, see **Fig. 17**. The Z-direction corresponds to the building direction. The cross-section samples were mounted in conductive resin and subsequently grinded and polished according to Struers standard

procedures for preparing stainless steel. The samples used for microstructure investigations were polished with 0.04 μm standard colloidal silica suspension (OP-S) and electrochemically etched in a 20 vol. % oxalic acid with a platinum electrode as counter cathode applying a potential of 3 V for 10 seconds.

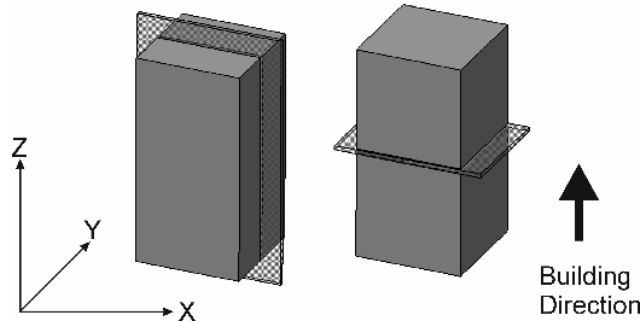


Figure 17: Planar cross-section of the prepared samples, z-plane (left) and XY-plane (right)

The powder cross-sections were studied on samples prepared by blending the powder together with the conductive resin which then was processed into metallographic samples according to Struers standard preparation routine. The samples were grounded and polished as the solid samples. The powder cross-sections were etched using Marble's Reagent (10g CuSO_4 , 50ml HCl and 50ml H_2O) to reveal the microstructural features. The powder samples for the SEM+EDX analysis were prepared by slightly pressing the powder onto a soft aluminum plate which then was mounted on a fixture in SEM instrument. The powder used for surface chemical analysis by XPS was mounted using carbon tape.

3.2 Light Optical Microscopy (LOM)

Light Optical Microscopy (LOM) collects reflected light through a set of lenses and generates an image of the investigated surface. In this study, a Leitz DMRX microscope was used with the AxioVison software for microstructural investigation and for porosity analysis in combination with the image analysis. The porosity investigation was performed on the polished samples and analyzed by a thresholding procedure using ImageJ, an image processing software.

3.3 Scanning Electron Microscopy (SEM)

Scanning electron microscopy (SEM) provides information about microstructural features and surface topography at high magnification with high spatial resolution. By directing the scanning electron beam through the electromagnetic lenses onto a sample surface, different types of radiations are generated as secondary electrons (SE), backscatter electrons (BSE) and X-rays, see **Fig. 18**. The radiations emitted at different depths of the surface will provide information about the surface characteristics and chemical composition, see **Fig. 18b**. In this study, microstructural features and surface topography of the powder and solid samples were investigated using SE imaging. Additionally, chemical analysis was performed using energy-dispersive X-ray spectroscopy (EDX), see **Fig. 18b and c**. However, due to the high interaction volume, only qualitative and semi-qualitative results were obtained regarding the chemical

composition since it was mainly used for examining small (less than $0.5\ \mu\text{m}$) particulates on the powder surfaces. The work presented in this thesis has been performed using a LEO Gemini 1550 (LEO GmbH, Oberkochen, Germany) scanning electron microscope equipped with an energy dispersive X-ray analyzer, X-Max (Oxford Instruments Ltd., HighWycombe, UK).

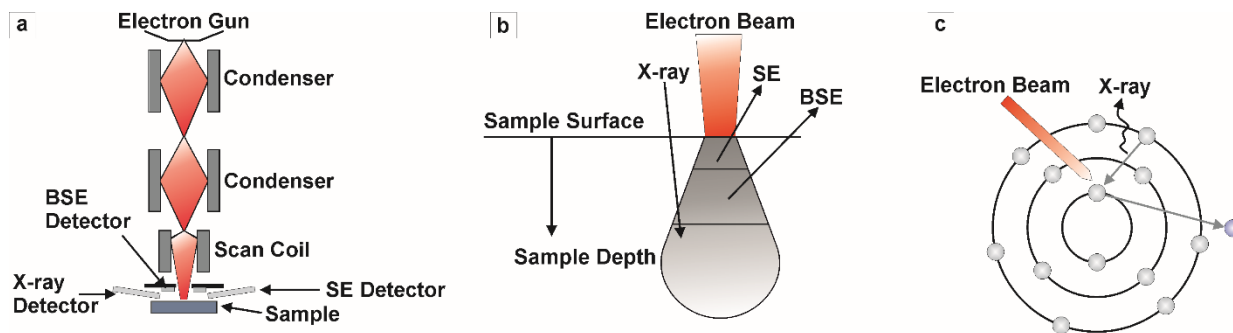


Figure 18: Schematic overview of a scanning electron microscope; (a) working principle, (b) interaction volume and (c) emission of X-rays

3.3.1 Electron Backscattered Diffraction (EBSD)

In paper III, crystallographic information was obtained by means of electron backscatter diffraction (EBSD). The generation of backscattered electrons was explained in section 3.3. By introducing a detector with a fluorescent screen, a diffraction pattern can be obtained and recorded. The recorded BSE produces a pattern known as Kikuchi bands. By analyzing the Kikuchi bands, a distinctive pattern can be identified that can give information about the orientation and crystal structures, the presence of local texturing, grains (orientation, boundaries and sizes) and phase composition, etc.

The EBSD can either be done as spot analysis or map analysis. To generate a map, the EBSD is measuring a point for a specific amount of time to gather the pattern and then moving one step size and making the next measurement, creating a raster grid of points which will produce an image with crystallographic orientations assigned to specific colors in the reconstructed image. Hence, smaller step sizes will generate a higher spatial resolution. By software processing, the results can be presented as inverse pole figures, where specific colors belong to a crystallographic grain of the same orientation or more specifically to the same lattice plane but since each plane can be rotated relative to one another, several planes can generate the same orientation.

The EBSD investigation presented in this thesis was performed with a Nordlys II detector (Oxford Instruments). An acceleration voltage of 20 keV was applied at a working distance of 10-20 mm with a step size between $0.05\text{-}3.0\ \mu\text{m}$. The EBSD maps were acquired and processed with Channel 5 software. Grain boundaries were defined to have a crystallographic misorientation of $>10^\circ$. All measurements were conducted on polished and etched samples.

3.4 X-ray Photoelectron Spectroscopy (XPS)

X-ray photoelectron spectroscopy (XPS) can be used for generating qualitative and quantitative information about the surface chemical state and composition. XPS is also known

as electron spectroscopy for chemical analysis (ESCA). A schematic overview is shown of the XPS method in **Fig. 19**. The XPS is a surface sensitive technique that measures the intensity of the emitted photoelectrons based on their binding energy and is able to detect almost all the elements, including light elements as e.g. O, C, N, etc. The most important characteristics of the XPS are high sensitivity, small analysis depth and the possibility to distinguish the chemical state of the elements. The photoelectrons are created by irradiating the sample with X-rays that penetrate the surface and interact with the atoms and generate photoelectrons. To enable a sufficient mean free path of the electrons after exiting the sample and to ensure that there is no contamination on the surface, the analysis needs to be performed in ultra-high vacuum. The X-ray photons are produced with a specific energy by using normally either Mg K α or Al K α sources. The energy of the emitted photoelectron is measured with a spectrometer and the intensity is measured in a specific energy channel. Elements are identified based on the unique binding energies for different photoelectron for given elements. The results are plotted with the number of emitted electrons per second against the binding energy (eV). Since the mean free path of a photoelectron is very small within the analyzed material, the detected photoelectrons will be generated from the outmost surface typically from 1-5 nm. A survey spectrum is used for general chemical composition analysis, which is based on a broad binding energy settings, while high energy resolution narrow scan measurements are used for determination of the chemical state, i.e. if an element is in the oxide or metallic state. The XPS analysis is usually first conducted on the as-received surface and by means alternating Ar $^{+}$ ion etching and analysis compositional depth profiling can be achieved.

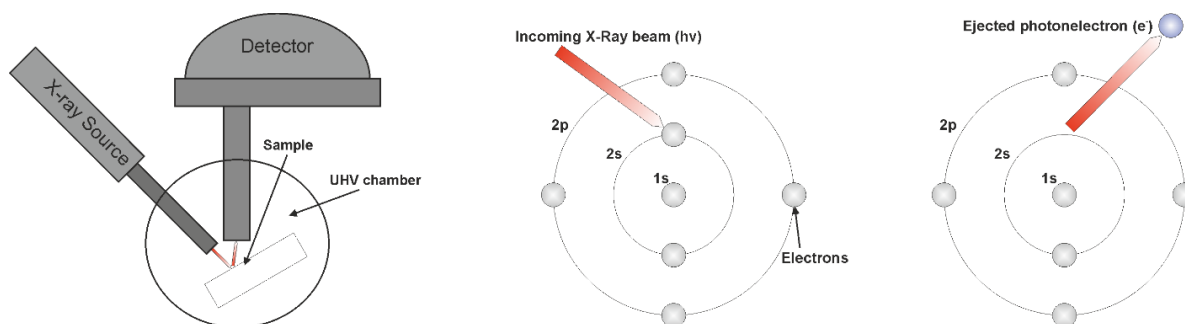


Figure 19: Schematic overview of the working principle of the XPS method.

In this study, the surface chemical composition of powder studied was analyzed using a PHI 5500 Spectrometer instrument equipped with monochromatic Al K α (1486.6 eV) X-ray source for photoelectron generation. The powder was mounted on a carbon tape for the analysis and the analyzed area was around 0.8 mm in diameter, based on the chosen aperture size. The acquisition conditions for high-energy spectra were 23.5 eV pass energy with the step of 0.1 eV and a nominal take-off angle of 45°. Curve fitting of the recorded photoelectron peaks was done utilizing the PHI Multipak software with asymmetric curves and assuming Shirley background [65]. Compositional depth profiling was done by alternating argon ion etching with an accelerating voltage of 4 kV, with an angle of 50° between the incident ion beam and the sample surface. The Ar $^{+}$ ions were rastered over an area of 4×5 mm 2 giving an etching rate of 3 nm min $^{-1}$. The etch rate was calibrated on a flat oxidized tantalum foil of 100 nm thickness. Hence the oxide thickness refers to Ta $_2$ O $_5$ units.

Chapter 4 - Results and Summary of Appended Papers

The results presented are based on the summary of the three appended papers. The paper I and Paper II are focused on the degradation of stainless steel powder associated with the PBF process. Characterization of both virgin and the recycled powder was conducted in order to establish an understanding of how the powder is affected by the PBF process. Paper III emphasizes the effect of the part geometry on the development of microstructure.

4.1 Powder degradation

Both kinds of virgin 316L powder showed a clear dendritic solidification structure, observed both on the particle surface and on the powder cross-section, see **Fig. 20**. The results from the powder recycling in the EBM process indicates that the homogenization takes place as a result of long-term exposure at high temperatures. The extent to which the homogenization happened depends on the location in the powder bed, as the time and temperature profile are different at different build height. Homogenization was not observed for powder recycled from the LBM. Since there is no preheating of the powder bed in the LBM process, the thermal history for the powder will depend on the distance from the built part and the built plate hold temperature, which is significantly lower than the temperatures used in EBM.

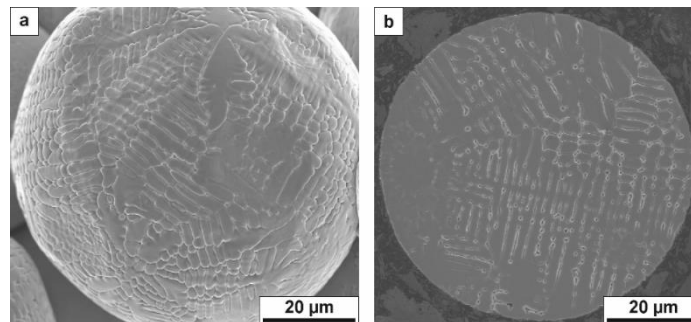


Figure 20: Microstructure of virgin powder showing a dendritic structure on the (a) surface and (b) cross-section of the powder.

Both kinds of powder studied are produced by well-controlled gas atomization processes and are of high quality, exhibiting smooth and clean surface with low amount of satellites. Still, at higher magnifications evenly distributed fine particulates were observed on the surface of the virgin powder as shown in **Fig. 21a and b**. The changes in the powder surface chemistry and morphology were clearly observed for the recycled powder when it comes to the morphology, size and amount of these particulates. Clear differences in powder degradation after EBM and LBM processing were observed as well, see **Fig. 21c and d**. The particulates on the powder surface in case of the LBM processed powder are darker and more spherical in shape and with size of up to 200 nm. The SEM+EDX analyses confirmed that they are rich in Cr, Mn, Si and Al combined with O. Meanwhile, the virgin powder used for EBM showed

particulates enriched in Si, Mn and Cr combined with O. Their size was estimated to be less than 50 nm. During the EBM process, the oxides grow in size up to ~150 nm while the surface of the powder used in LBM process appeared to be much less affected.

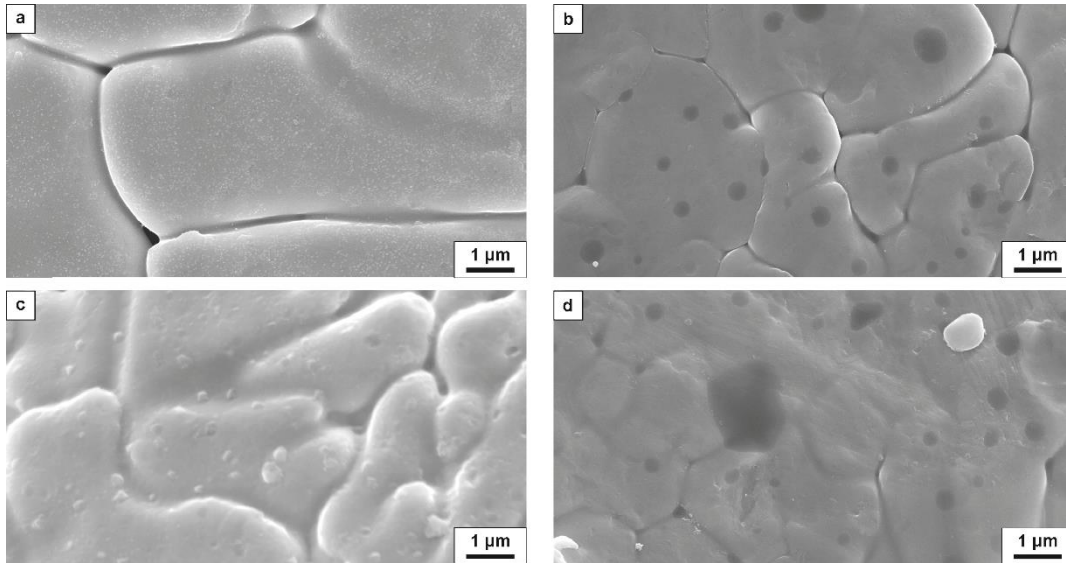


Figure 21: The particulate features on the powder surface from (a) virgin 316LN (EBM), (b) virgin 316L (LBM), (c) recycled 316LN (EBM) and (d) recycled 316L (LBM).

The surface chemical composition was measured on the EBM-processed powder by means of XPS depth profiling. The chemical composition of the outermost surface and down to 50 nm was measured. A steep decrease in oxygen was observed with increased Fe content for etch depth down to about 7.5 nm. As shown in **Fig. 22**, the surface enrichment in Cr and Mn (in oxide state) in combination with high residual oxygen content at larger etch depths confirm the presence of particulate oxides features observed by SEM. The main difference is that the recycled powder had a lower amount of Mn, which is supposed to be connected to the sublimation of Mn at high temperature during EBM processing (and hence reduction of Mn-oxide). The results show that the surface of the powder undergoes changes in terms of chemical composition with a decrease in oxide layer thickness and an increased amount of Cr-Mn rich oxides particulates.

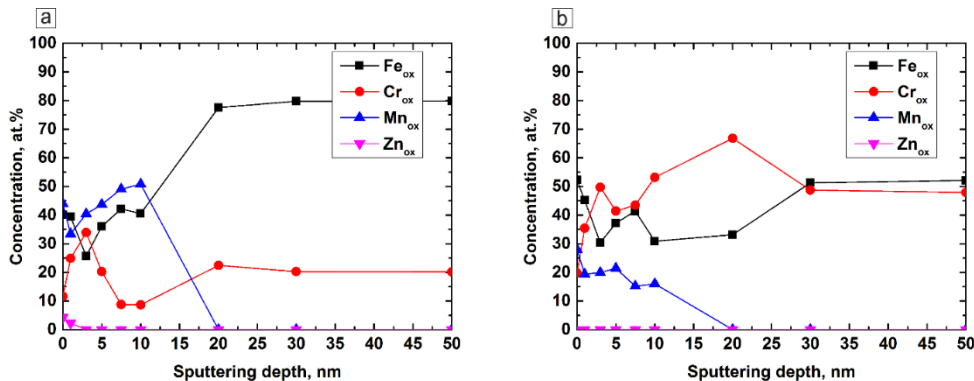


Figure 22: Relative cation concentration of the surface of (a) the virgin powder and (b) the recycled 316LN powder used in EBM

4.2 Microstructure

In order to investigate how part design affects the microstructure, samples with different rib thicknesses and build inclination were fabricated. The results revealed that by appropriate design, ribs with 0.2 mm thickness could be successfully fabricated without failure. Moreover, it was shown that ribs with a build angle of 30° were successfully built without support structures. However, with inferior surface roughness and poor dimensional accuracy.

The produced samples were investigated in an as-built condition and the cross-section showed a complex solidification structure, as shown in **Fig. 23**. This type of solidification structures is commonly observed in stainless steel part fabricated by PBF as described in section 2.5. As shown in **Fig. 23**, the melt pool boundaries are clearly distinguished and are around 100-200 μm in a width and 25-100 μm in depth. The depth of the melt pool is larger than the layer thickness, meaning that the laser has thermally affected more than one layer and therefore re-melting of previous layers has occurred. This ensures that the parts were fully consolidated without large defects and/or lack of fusion regions. Analysis of un-etched samples indicated that almost full density (over 99.9 %) was achieved independent on rib thickness or build inclination. Hence no correlation between rib thickness and porosity was observed.

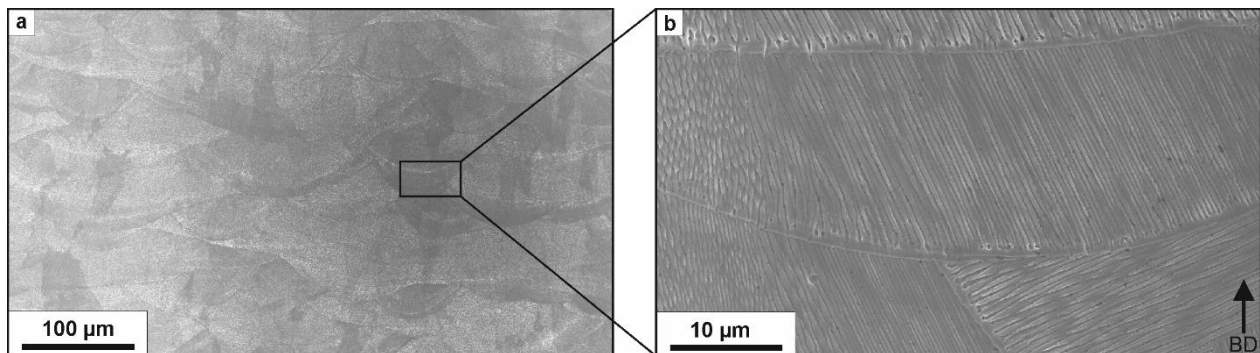


Figure 23: SEM image of the cross-section of the as-built AM parts at (a) low magnification and (b) higher magnification.

The microstructure of the ribs was investigated by EBSD in order to provide information about the grain morphology and texture in the components. The EBSD orientation maps indicated that the microstructure consists of large elongated grains which covers several built layers and melt pool boundaries as shown in **Fig. 24a**. The grains were growing in an epitaxial manner following the building direction with a preferential $\langle 101 \rangle$ orientation. Furthermore, close to the part surface smaller grains were observed. The small grains had grown inwards, towards the rib center, following the maximum temperature gradient. This tendency was observed to $\sim 150 \mu\text{m}$ from the part surface after which large elongated grains were shaped. For the thinnest ribs (0.2 and 0.4 mm) these small inclined grains were covering the full thickness as shown in **Fig. 24b**. The small grains were randomly oriented in contrast to the large elongated grains. The small grains were assumed to be formed due to an increased cooling rate closer to the part surface. The increased cooling rate is supposed to hinder grain growth and change the preferential grain orientation. Furthermore, the ribs which were fabricated with a build angle indicated that the grains are still elongated in the building direction rather than being affected by the part geometry, as shown in see **Fig. 25**. The inclined ribs had a random texture in contrast to the straight ribs which had a predominant

$\langle 101 \rangle$ orientation. Close to the surface of the inclined samples small grains were observed, similar to what was observed in the straight ribs. However, the grains are instead directed in the same direction as the part.

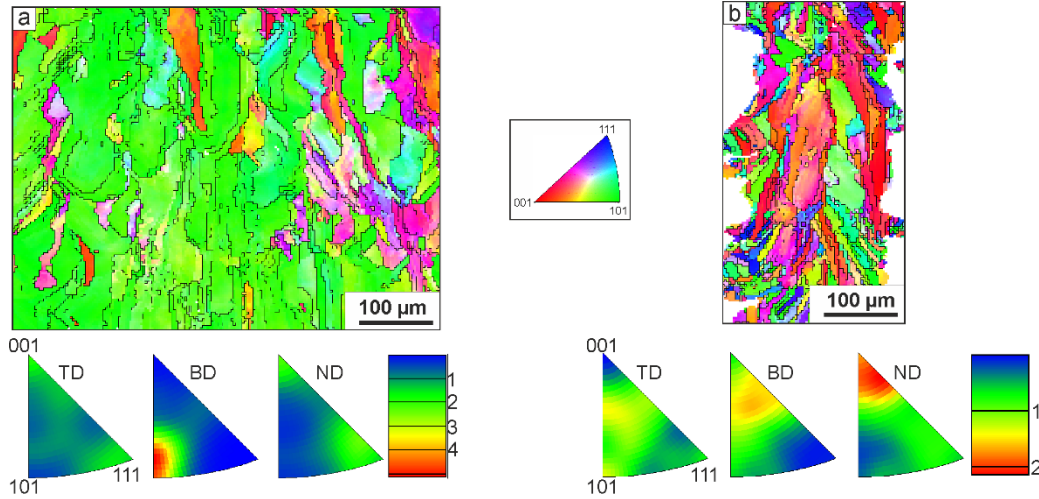


Figure 24: EBSD orientation maps with inverse pole figure coloring of (a) 1 mm rib and (b) 0.2 mm rib. Provided are also the inverse pole figure color code and the inverse pole figures in (transverse direction (TD), building direction (BD), and normal direction (ND)).

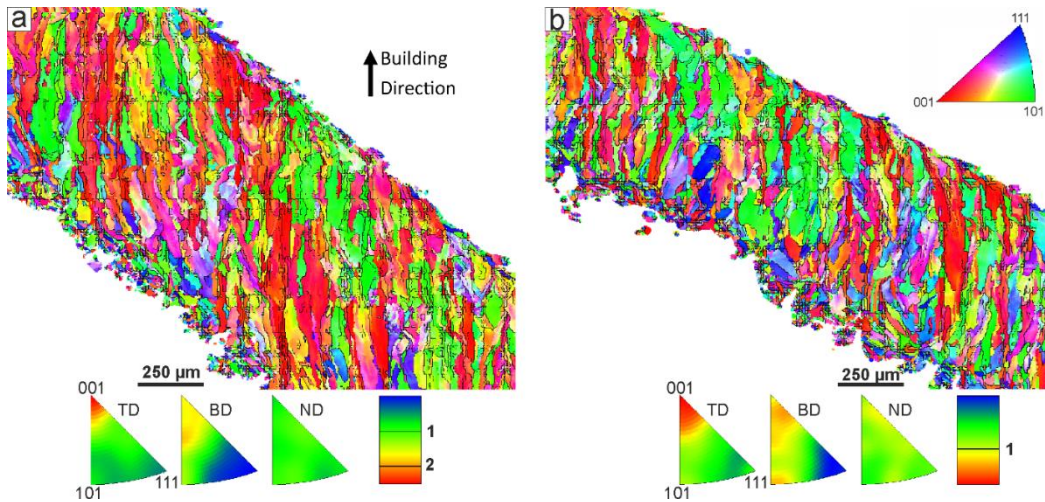


Figure 25: EBSD orientation maps of different build inclinations (a) 45° and (b) 30°.

Chapter 5 - Summary and Conclusions

The aim of this licentiate thesis study was to provide improved understanding how to ensure a robust production of stainless steel when utilizing PBF and to recognize the link between feedstock materials, build geometry, process and part quality. The results relate to several aspects that are supposed to influence the final outcome, including pre- and post-processing, quality of feedstock material, build orientation and part design.

To have an economically feasible PBF process, powder recycling is a necessity. However, to ensure a robust process and consistent material properties, the feedstock material needs to be handled with caution. Improper powder handling is expected to affect the part quality owing to changes in powder characteristics like size distribution, morphology, flowability and chemical composition. This study has proven the degradation of 316L stainless steel powder in terms of surface chemistry changes in case of recycled powder. It was revealed that both recycled and virgin powders were covered by a heterogeneous oxide layer, composed of homogeneous iron oxide layer with the presence of Cr-Mn-rich oxide particulates. These particulates were growing during PBF processing, but were most pronounced in the EBM process. However, the effect of the powder degradation on the component properties is still not clear and should be further investigated to ensure that proper powder handling can be further established. Furthermore, the powder degradation was shown to depend on the PBF process employed, where the EBM process affected the powder more strongly, compared to LBM, due to the longer exposure at high temperatures.

The PBF process offers almost unlimited design freedom but utilization of its full potential requires knowledge of how different designs affects the microstructure. In this study, ribs of different thicknesses and build angles were fabricated in order to understand how the microstructure is affected by some basic geometrical features. The PBF process produces a complex microstructure with large elongated grains oriented in the building direction. The results of this investigation show that close to the part surface ($\sim 150 \mu\text{m}$) smaller grains are formed. These grains are inclined towards the center of the part and have random orientation in contrast to the large elongated grains in the center of the part, which has a preferential $\langle 101 \rangle$ orientation. Hence, the results indicate that wall thickness smaller than 0.6 mm will have a microstructure consisting of only the small more equiaxed grains with random orientation. Above 0.6 mm wall thickness, a core of large elongated grains will start to form in the center of the part. Furthermore, by decreasing the building angle to 45° and 30° for 1 mm thick ribs resulted in grains with a random orientation. However, the microstructure still contained large elongated grains that followed the building direction, as in the straight ribs. Hence, the grain growth direction was not affected by the build angle.

In conclusion, to ensure high-quality components manufactured by powder bed fusion, the whole process needs to be well-controlled. To ensure good reproducibility, more extensive recycling studies need to be conducted in combination with mechanical testing. Furthermore, it is reasonable to assume that mechanical properties will change by reducing the wall thickness owing to the changes in grain size and texture. Therefore, dedicated mechanical testing will be needed to further understand the impact of thin walled structures and build orientation.

Acknowledgements

First I would like to thank my supervisor Prof. Eduard Hryha for giving me the opportunity to work with this growing and exciting topic and for his guidance. Further, my co-supervisor Lars Nyborg is greatly acknowledged for his input, guidance and help throughout the work.

I would like to express my gratitude to Prof. Uta Klement for her support and feedback.

I also would like to acknowledge the research engineers Dr. Ruslan Shvab, Dr. Eric Tam, Dr. Yiming Yao, Dr. Yu Cao, Lic. Eng. Lars Hammar and Roger Sagdahl for their help regarding all practical work.

Lars-Erik Rännar and Andrey Koptuyug from Mid Sweden University are acknowledged their help with the EBM processing and powder sampling used in this work.

Financial support from Vinnova within the framework of the Metallic Materials programme, AoA Production at Chalmers, Fusion for Energy through the grant GRT-645, Västragötalandsregionen and Tillväxtverket is gratefully acknowledged. The results and conclusions in this thesis report are provided by the author and Fusion for Energy is not held responsible for any of these results or conclusions.

Recognitions to all the colleagues at the Department of Industrial and Materials Science for making the time enjoyable.

I would like to thank Camille, Dmitri, Eric, Hans, Johan, Maheswaran, Mikael and Swathi for all the discussion, ideas, and memorable stories created during our conferences.

I would like to thank my family and friends for reminding me of the world outside the office.

Finally, thanks to Linn and Edvin for their boundless love and support throughout this journey.

References

- [1] ASTM International, F2792-12a - Standard Terminology for Additive Manufacturing Technologies, Rapid Manuf. Assoc. (2013) 10–12. doi:10.1520/F2792-12A.2.
- [2] L.-E. Rännar, A. Koptuyug, J. Olsén, K. Saeidi, Z. Shen, Hierarchical structures of stainless steel 316L manufactured by Electron Beam Melting, *Addit. Manuf.* (2017). doi:10.1016/j.addma.2017.07.003.
- [3] Y. Zhong, L.-E. Rännar, L. Liu, A. Koptuyug, S. Wikman, J. Olsen, D. Cui, Z. Shen, Additive manufacturing of 316L stainless steel by electron beam melting for nuclear fusion applications, *J. Nucl. Mater.* 486 (2017) 234–245. doi:10.1016/j.jnucmat.2016.12.042.
- [4] J. Technik, Injection mold cooling configuration, (2010) 71–74. <http://acta.fih.upt.ro/pdf/2010-1/ACTA-2010-1-12.pdf>.
- [5] L. Wang, Q.S. Wei, P.J. Xue, Y.S. Shi, Fabricate Mould Insert with Conformal Cooling Channel Using Selective Laser Melting, *Adv. Mater. Res.* 502 (2012) 67–71. doi:10.4028/www.scientific.net/AMR.502.67.
- [6] D. Gu, Laser Additive Manufacturing of High-Performance Materials, n.d.
- [7] D. Wang, C. Song, Y. Yang, Y. Bai, Investigation of crystal growth mechanism during selective laser melting and mechanical property characterization of 316L stainless steel parts, *Mater. Des.* 100 (2016) 291–299. doi:10.1016/j.matdes.2016.03.111.
- [8] A.B. Spierings, G. Levy, Comparison of density of stainless steel 316L parts produced with selective laser melting using different powder grades, *Solid Free. Fabr. Proc.* (2009) 342–353.
- [9] C.T. Schade, T.F. Murphy, C. Walton, Development of atomized powders for additive manufacturing, *World Congr. Powder Metall. Part. Mater. PM 2014*, May 18, 2014 - May 22, 2014. (2014) 215–226.
- [10] Y.Y. Sun, S. Gulizia, C.H. Oh, C. Doblin, Y.F. Yang, M. Qian, Manipulation and Characterization of a Novel Titanium Powder Precursor for Additive Manufacturing Applications, *Jom.* 67 (2015) 564–572. doi:10.1007/s11837-015-1301-3.
- [11] B. Liu, R. Wildman, C. Tuck, I. Ashcroft, R. Hague, Investigation the Effect of Particle Size Distribution on Processing Parameters Optimisation in Selective Laser Melting Process, *Sff.* (2011) 227–238. doi:10.1017/CBO9781107415324.004.
- [12] J. Karlsson, A. Snis, H. Engqvist, J. Lausmaa, Characterization and comparison of materials produced by Electron Beam Melting (EBM) of two different Ti-6Al-4V powder fractions, *J. Mater. Process. Technol.* 213 (2013) 2109–2118. doi:10.1016/j.jmatprotec.2013.06.010.
- [13] A. Strondl, O. Lyckfeldt, H. Brodin, U. Ackelid, Characterization and Control of Powder Properties for Additive Manufacturing, *Jom.* 67 (2015) 549–554. doi:10.1007/s11837-015-1304-0.
- [14] J.M. Benson, E. Snyders, the Need for Powder Characterisation in the Additive Manufacturing, *South African J. Ind. Eng.* 26 (2015) 104–114.
- [15] M. Schmid, F. Amado, G. Levy, K. Wegener, Flowability of powders for Selective Laser Sintering (SLS) investigated by Round Robin Test, *High Value Manuf. Adv.*

- Res. Virtual Rapid Prototyp. - Proc. 6th Int. Conf. Adv. Res. Rapid Prototyping, VR@P 2013. (2014) 95–99. doi:10.1201/b15961-19.
- [16] A. Cooke, J. Slotwinski, Properties of metal powders for additive manufacturing: A review of the state of the art of metal powder property testing, *Addit. Manuf. Mater. Stand. Test. Appl.* (2015) 21–48. doi:10.6028/NIST.IR.7873.
- [17] A.B. Spierings, N. Herres, G. Levy, Influence of the particle size distribution on surface quality and mechanical properties in additive manufactured stainless steel parts, 21st Annu. Int. Solid Free. Fabr. Symp. - An Addit. Manuf. Conf. SFF 2010, August 9, 2010 - August 11, 2010. (2010) 397–406. doi:10.1108/13552541111124770.
- [18] A.T. Sutton, C.S. Kriewall, M.C. Leu, J.W. Newkirk, Powder characterisation techniques and effects of powder characteristics on part properties in powder-bed fusion processes, *Virtual Phys. Prototyp.* 2759 (2016) 1–27. doi:10.1080/17452759.2016.1250605.
- [19] R. Li, Y. Shi, Z. Wang, L. Wang, J. Liu, W. Jiang, Densification behavior of gas and water atomized 316L stainless steel powder during selective laser melting, *Appl. Surf. Sci.* 256 (2010) 4350–4356. doi:10.1016/j.apsusc.2010.02.030.
- [20] L.C. Ardila, F. Garciandia, J.B. Gonzalez-Diaz, P. Alvarez, A. Echeverria, M.M. Petite, R. Deffley, J. Ochoa, Effect of IN718 recycled powder reuse on properties of parts manufactured by means of Selective Laser Melting, *Phys. Procedia.* 56 (2014) 99–107. doi:10.1016/j.phpro.2014.08.152.
- [21] V. Manakari, G. Parande, M. Gupta, H.F. Lopez, Selective Laser Melting of Magnesium and Magnesium Alloy Powders : A Review, 2017. doi:10.3390/met7010002.
- [22] C. Körner, Additive manufacturing of metallic components by selective electron beam melting — a review, *Int. Mater. Rev.* 61 (2016) 361–377. doi:10.1080/09506608.2016.1176289.
- [23] S. Das, On Some Physical Aspects of Process Control in Direct Selective Laser Sintering of Metals: Part 1, *Solid Free. Fabr. Symp.* (2001) 85–93.
- [24] W.J. Sames, F.A. List, S. Pannala, R.R. Dehoff, S.S. Babu, The metallurgy and processing science of metal additive manufacturing, *Int. Mater. Rev.* 6608 (2016) 1–46. doi:10.1080/09506608.2015.1116649.
- [25] S. Matthes, R. Kahlenberg, S. Jahn, C. Straube, About the Influence of powder properties on the Selective Laser Melting Process, *Fraunhofer Direct Digit. Manuf. Conf.* (2016) 1–5.
- [26] E. Hryha, C. Gierl, L. Nyborg, H. Danninger, E. Dudrova, Surface composition of the steel powders pre-alloyed with manganese, *Appl. Surf. Sci.* 256 (2010) 3946–3961. doi:10.1016/j.apsusc.2010.01.055.
- [27] V. Petrovic, R. Niñerola, Powder recyclability in electron beam melting for aeronautical use, *Aircr. Eng. Aerosp. Technol.* 87 (2015) 147–155. doi:10.1108/AEAT-11-2013-0212.
- [28] P. Nandwana, W.H. Peter, R.R. Dehoff, L.E. Lowe, M.M. Kirka, F. Medina, S.S. Babu, Recyclability Study on Inconel 718 and Ti-6Al-4V Powders for Use in Electron Beam Melting, *J. Dyn. Differ. Equations.* (2015). doi:10.1007/s10884-015-9497-z.
- [29] R. Shvab, A. Leicht, E. Hryha, L. Nyborg, Characterization of the virgin and recycled nickel alloy HX powder used for selective laser melting, *Proc. WorldPM2016.* (2016).
- [30] H.P. Tang, M. Qian, N. Liu, X.Z. Zhang, G.Y. Yang, J. Wang, Effect of Powder Reuse Times on Additive Manufacturing of Ti-6Al-4V by Selective Electron Beam Melting, *Jom.* 67 (2015) 555–563. doi:10.1007/s11837-015-1300-4.
- [31] R. O’Leary, R. Setchi, P. Prickett, G. Hankins, N. Jones, An Investigation into the

- Recycling of Ti-6Al-4V Powder Used Within SLM to Improve Sustainability, SDM'2015 2nd Int. Conf. Sustain. Des. Manuf. , (2015) 14–17.
- [32] J. a Slotwinski, S.S. Watson, P.E. Stutzman, C.F. Ferraris, M. a Peltz, E.J. Garboczi, Application of physical and chemical characterization techniques to metallic powders, 40th Annu. Rev. Prog. Quant. Nondestruct. Eval. QNDE 2013, Inc. 10th Int. Conf. Barkhausen Micro-Magnetics, ICBM 2013. 1581 33 (2014) 1184–1190. doi:10.1063/1.4864955.
- [33] S. Berretta, O. Ghita, K.E. Evans, A. Anderson, C. Newman, Size, shape and flow of powders for use in Selective Laser Sintering (SLS), 6th Int. Conf. Adv. Res. Virtual Phys. Prototyping, VR@P 2013, Oct. 1, 2013 - Oct. 5, 2013. (2014) 49–54.
- [34] E. Louvis, P. Fox, C.J. Sutcliffe, Selective laser melting of aluminium components, J. Mater. Process. Technol. 211 (2011) 275–284. doi:10.1016/j.jmatprotec.2010.09.019.
- [35] M.S.F. de Lima, S. Sankaré, Microstructure and mechanical behavior of laser additive manufactured AISI 316 stainless steel stringers, Mater. Des. 55 (2014) 526–532. doi:10.1016/j.matdes.2013.10.016.
- [36] T. Niendorf, S. Leuders, A. Riemer, H.A. Richard, T. Tröster, D. Schwarze, Highly anisotropic steel processed by selective laser melting, Metall. Mater. Trans. B Process Metall. Mater. Process. Sci. 44 (2013) 794–796. doi:10.1007/s11663-013-9875-z.
- [37] Z. Sun, X. Tan, S.B. Tor, W.Y. Yeong, Selective laser melting of stainless steel 316L with low porosity and high build rates, Mater. Des. 104 (2016) 197–204. doi:10.1016/j.matdes.2016.05.035.
- [38] A. R??ttger, K. Geenen, M. Windmann, F. Binner, W. Theisen, Comparison of microstructure and mechanical properties of 316 L austenitic steel processed by selective laser melting with hot-isostatic pressed and cast material, Mater. Sci. Eng. A. 678 (2016) 365–376. doi:10.1016/j.msea.2016.10.012.
- [39] I. Yadroitsev, P. Krakhmalev, I. Yadroitsava, S. Johansson, I. Smurov, Energy input effect on morphology and microstructure of selective laser melting single track from metallic powder, J. Mater. Process. Technol. 213 (2013) 606–613. doi:10.1016/j.jmatprotec.2012.11.014.
- [40] J.D. Majumdar, A. Pinkerton, Z. Liu, I. Manna, L. Li, Microstructure characterisation and process optimization of laser assisted rapid fabrication of 316L stainless steel, Appl. Surf. Sci. 247 (2005) 320–327. doi:10.1016/j.apsusc.2005.01.039.
- [41] E. Yasa, J.-P.P. Kruth, Microstructural investigation of selective laser melting 316L stainless steel parts exposed to laser re-melting, Procedia Eng. 19 (2011) 389–395. doi:10.1016/j.proeng.2011.11.130.
- [42] A.I. Mertens, S. Reginster, Q. Contrepois, T. Dormal, O. Lemaire, J. Lecomte-Beckers, Mechanical properties of alloy Ti–6Al–4V and of stainless steel 316L processed by selective laser melting: influence of out-of-equilibrium microstructures, Mater. Sci. Forum. 783–786 (2014) 898–903. doi:10.4028/www.scientific.net/MSF.783-786.898.
- [43] Y. Zhong, L. Liu, S. Wikman, D. Cui, Z. Shen, Intragranular cellular segregation network structure strengthening 316L stainless steel prepared by selective laser melting, J. Nucl. Mater. 470 (2016) 170–178. doi:10.1016/j.jnucmat.2015.12.034.
- [44] L. Thijs, K. Kempen, J.P. Kruth, J. Van Humbeeck, Fine-structured aluminium products with controllable texture by selective laser melting of pre-alloyed AlSi10Mg powder, Acta Mater. 61 (2013) 1809–1819. doi:10.1016/j.actamat.2012.11.052.
- [45] K. Saeidi, X. Gao, Y. Zhong, Z.J. Shen, Hardened austenite steel with columnar sub-grain structure formed by laser melting, Mater. Sci. Eng. A. 625 (2015) 221–229. doi:10.1016/j.msea.2014.12.018.
- [46] J.A. Cherry, H.M. Davies, S. Mehmood, N.P. Lavery, S.G.R. Brown, J. Sienz,

- Investigation into the effect of process parameters on microstructural and physical properties of 316L stainless steel parts by selective laser melting, *Int. J. Adv. Manuf. Technol.* 76 (2015) 869–879. doi:10.1007/s00170-014-6297-2.
- [47] D. Wang, C. Song, Y. Yang, Y. Bai, Investigation of crystal growth mechanism during selective laser melting and mechanical property characterization of 316L stainless steel parts, *Mater. Des.* 100 (2016) 291–299. doi:10.1016/j.matdes.2016.03.111.
- [48] R. Casati, J. Lemke, M. Vedani, Microstructure and Fracture Behavior of 316L Austenitic Stainless Steel Produced by Selective Laser Melting, *J. Mater. Sci. Technol.* 32 (2016) 738–744. doi:10.1016/j.jmst.2016.06.016.
- [49] K. Saeidi, X. Gao, F. Lofaj, L. Kvetková, Z.J.J. Shen, Transformation of austenite to duplex austenite-ferrite assembly in annealed stainless steel 316L consolidated by laser melting, *J. Alloys Compd.* 633 (2015) 463–469. doi:10.1016/j.jallcom.2015.01.249.
- [50] M.L. Pace, A. Guarnaccio, P. Dolce, D. Mollica, G.P. Parisi, A. Lettino, L. Medici, V. Summa, R. Ciancio, A. Santagata, 3D additive manufactured 316L components microstructural features and changes induced by working life cycles, *Appl. Surf. Sci.* (2017) 1–9. doi:10.1016/j.apsusc.2017.01.308.
- [51] L.-E. Rännar, A. Koptuyug, J. Olsén, K. Saeidi, Z. Shen, Hierarchical structures of stainless steel 316L manufactured by Electron Beam Melting, *Addit. Manuf.* 17 (2017) 106–112. doi:10.1016/j.addma.2017.07.003.
- [52] T.M. Mower, M.J. Long, Mechanical behavior of additive manufactured, powder-bed laser-fused materials, *Mater. Sci. Eng. A.* 651 (2016) 198–213. doi:10.1016/j.msea.2015.10.068.
- [53] W. Shifeng, L. Shuai, W. Qingsong, C. Yan, Z. Sheng, S. Yusheng, Effect of molten pool boundaries on the mechanical properties of selective laser melting parts, *J. Mater. Process. Technol.* 214 (2014) 2660–2667. doi:10.1016/j.jmatprotec.2014.06.002.
- [54] D. Wang, Y. Yang, X. Su, Y. Chen, Study on energy input and its influences on single-track, multi-track, and multi-layer in SLM, *Int. J. Adv. Manuf. Technol.* 58 (2012) 1189–1199. doi:10.1007/s00170-011-3443-y.
- [55] A. Riemer, S. Leuders, M. Thöne, H.A.A. Richard, T. Tröster, T. Niendorf, On the fatigue crack growth behavior in 316L stainless steel manufactured by selective laser melting, *Eng. Fract. Mech.* 120 (2014) 15–25. doi:10.1016/j.engfracmech.2014.03.008.
- [56] C. Puzon, E. Hryha, P. Forêt, L. Nyborg, Effect of Argon and Nitrogen Atmospheres on the Properties of the As-Built 316L Stainless Steel Components by Laser Sintering, (n.d.) 2–8.
- [57] M. Anne, S. Reginster, H. Paydas, Q. Contrepolis, T. Dormal, O. Lemaire, J. Lecomte-Beckers, A. Mertens, S. Reginster, H. Paydas, Q. Contrepolis, T. Dormal, O. Lemaire, J. Lecomte-Beckers, Mechanical properties of alloy Ti–6Al–4V and of stainless steel 316L processed by selective laser melting: influence of out-of-equilibrium microstructures, *Powder Metall.* 57 (2014) 184–189. doi:10.1179/1743290114Y.0000000092.
- [58] E. Sallica-Leva, A.L. Jardini, J.B. Fogagnolo, Microstructure and mechanical behavior of porous Ti–6Al–4V parts obtained by selective laser melting, *J. Mech. Behav. Biomed. Mater.* 26 (2013) 98–108. doi:10.1016/j.jmbbm.2013.05.011.
- [59] K.S. Chan, M. Koike, R.L. Mason, T. Okabe, Fatigue life of titanium alloys fabricated by additive layer manufacturing techniques for dental implants, *Metall. Mater. Trans. A Phys. Metall. Mater. Sci.* 44 (2013) 1010–1022. doi:10.1007/s11661-012-1470-4.
- [60] K. Alrbaey, D. Wimpenny, R. Tosi, W. Manning, A. Moroz, On optimization of surface

- roughness of selective laser melted stainless steel parts: A statistical study, *J. Mater. Eng. Perform.* 23 (2014) 2139–2148. doi:10.1007/s11665-014-0993-9.
- [61] D. Wang, Y. Liu, Y. Yang, D. Xiao, Theoretical and experimental study on surface roughness of 316L stainless steel metal parts, *Rapid Prototyp. J.* 22 (2016) 706–716. doi:10.1108/RPJ-06-2015-0078.
- [62] J. Timhagen, D. Nalum, Study of wall thickness and its impact on microstructure on 316L manufactured with Direct Metal Laser Sintering, (2017).
- [63] European Powder Metallurgy Association, Introduction to additive manufacturing technology, (2 nd). acc:www.epma.com/am (2017).
- [64] J. Kranz, D. Herzog, C. Emmelmann, Design guidelines for laser additive manufacturing of lightweight structures in TiAl6V4, *J. Laser Appl.* 27 (2015) S14001. doi:10.2351/1.4885235.
- [65] E. Hryha, R. Shvab, M. Bram, M. Bitzer, L. Nyborg, Surface chemical state of Ti powders and its alloys: Effect of storage conditions and alloy composition, *Appl. Surf. Sci.* 388 (2016) 294–303. doi:10.1016/j.apsusc.2016.01.046.